SIGNATURES OF THE HIGGS BOSON THROUGH ITS PRODUCTION IN ASSOCIATION WITH A TOP QUARK PAIR

By

SOMNATH BANDYOPADHYAY

Enrollment No: PHYS07200604012

Institute of Physics
Bhubaneswar - 751005, India

A thesis submitted to
The Board of Studies in Physical Sciences

In partial fulfillment of requirements

For the Degree of

DOCTOR OF PHILOSOPHY

of

HOMI BHABHA NATIONAL INSTITUTE

October, 2014

Homi Bhabha National Institute

Recommendations of the Viva Voce Board

As members of the Viva Voce Board, we certify that we have read the dissertation prepared by Mr. **Somnath Bandyopadhyay**, entitled "**Signatures of the Higgs Boson Through its Production in Association with a Top Quark Pair**", and recommend that it may be accepted as fulfilling the dissertation requirement for the Degree of Doctor of Philosophy.

Ajit M. Srivastava -- **Date:** 30/12/15

Chairman - (Prof. Ajit M. Srivastava)

Pankaj Agrawal -- **Date:** 30-12-15

Guide / Convener – (Prof. Pankaj Agrawal)

-- **Date:** 30/12/15

Member 1 - (Prof. Sudhir K. Vempati)

-- **Date:** 30/12/2015

Member 2 - (Prof. Suresh K. Patra)

-- **Date:** 30/12/2015

Member 3 - (Prof. Tapobrata Som)

Final approval and acceptance of this dissertation is contingent upon the candidate's submission of the final copies of the dissertation to HBNI.

I hereby certify that I have read this dissertation prepared under my direction and recommend that it may be accepted as fulfilling the dissertation requirement.

Date: 30-12-15

Place: Bhubaneswar

Pankaj Agrawal

(PANKAJ AGRAWAL)

STATEMENT BY AUTHOR

This dissertation has been submitted in partial fulfillment of requirements for an advanced degree at Homi Bhabha National Institute (HBNI) and is deposited in the Library to be made available to borrowers under rules of the HBNI. Brief quotation from this dissertation are allowable without special permission, provided that accurate acknowledgment of source is made. Requests for permission for extended quotation from or reproduction of this manuscript in whole or in part may be granted by the Competent Authority of HBNI when in his or her judgment the proposed use of the material is in the interests of scholarship. In all other instances, however, permission must be obtained from the author.

Somnath Bandyopadhyay

DECLARATION

I, Somnath Bandyopadhyay, hereby declare that the investigation presented in the thesis has been carried out by me. The work is original and has not been submitted earlier as a whole or in part for a degree/diploma at this or any other Institution/University.

Somnath Bandyopadhyay

CERTIFICATE

This is to certify that the thesis entitled **"SIGNATURES OF THE HIGGS BOSON THROUGH ITS PRODUCTION IN ASSOCIATION WITH A TOP QUARK PAIR"**, which is being submitted by **Mr. Somnath Bandyopadhyay**, in partial fulfillment of the degree of **Doctor of Philosophy in physics** of **Homi Bhabha National Institute** is a record of his own research work carried by him. He has carried out his investigations on the subject of matter of the thesis under my supervision at **Institute of Physics, Bhubaneswar**. To the best of our knowledge, the matter embodied in this thesis has not been submitted for the award of any other degree.

Signature of the candidate
(Somnath Bandyopadhyay)

Signature of the supervisor
(Prof. Pankaj Agrawal)

Dedicated to my family

Contents

Acknowledgement

This thesis has been possible due to support, advice, encouragement, friendship and affection of many people.

First, I would like to thank **Prof. Pankaj Agrawal**, my thesis supervisor for his invaluable guidance, encouragement and his constant support throughout my research period at the Institute. He has been the constant source of inspiration all along the way. I have learnt a lot from him not only about physics but also about life in general. I heartily thank him and his family for making my stay comfortable in the Institute.

The thanks giving will be incomplete without mentioning name of my collaborator, Dr. Siba Prasad Das. I really owe to him.

I must mention that, one of the most interesting, knowledgeable and difficult course I have attend is the Pre-Doctoral course at IOP. I would like to thank all my teachers who taught me during the Pre-doctoral course and other faculty members of IOP. Special thanks goes to Dr. Topabrata Som, Dr. Suresh Kumar Patro, Dr. Biju Raj Shekhar, Dr. Durga Prasad Mohapatra and Dr. P.V.Satyam.

I would like thank my committee members Dr. Avinash Khare and Dr. Ajit Mohan Srivastav whose valuable comments always help me to do better. Dr. Ajit Mohan Srivastava also helped me a lot as dean of HBNI in IOP. I am extremely thankful for his help. I would also like to thank all the members of Theoretical Physics Group at Institute of Physics for helping me in understanding various aspects of Physics in general.

It would like to thank my seniors, scholar friends and others, they include, Zashmir whose time to time help to understand my subject helped me a lot. I would also like to thank Manas Dalai, Ananta Prasad Mishra, Sinu Mathew, Boby, Partho etc to make my stay pleasurable in the campus. My sincere thanks goes to my friends Janmejaya Mishra and Jayanta Mishra for their love for me.

I am also thankful to Surasree Mazumder and Souvik Banerjee to give me the format of thesis and help me to type the thesis.

It will be impossible for me to forget the picnics, pujas, cricket matches, tennis matches and dinner-lunch-breakfast-tea time gossips with them. I thank them for all their direct and indirect help throughout my stay at IOP.

I would like to express my sincere thanks to Dr. Arum M. Jayannavar, Ex-Director, IOP. I am also thankful to all the staff members of the beautiful IOP library, the people who have maintained our computer center and all the administrative and non-academic staff of IOP, for their support, co-operation and help at every stage.

At last the acknowledgment will not be complete without thanking some of the administrative staff. They include our Registrar Mr. Chandra Bhanu Mishra, and Mr. Bir Kishore Mishra. Mr. Ramanuja Sarangi deservs special thanks to help me out in my bad time.

My humble regards, respect and thanks goes to my parents, sister, brother and other family members for their patience and encouragement during my research period. It is because of their love, affection and blessings that I could complete this thesis.

At last but not least I would like to thanks **ALMIGHTY**, without whose blessings the project may not have completed.

Date:

(Somnath Bandyopadhyay)

Synopsis

The matter around us is made up of basic building blocks known as quarks and leptons. Each of the group of quarks contains six particles and are further divided into three pairs called generations. The lightest of the particles, which are also most stable, form the first generations. While the heaviest and the most unstable, form the third generation. The second generation is moderately heavy and moderately unstable. The first generation quarks are up quark and down quark. The second and the third generations are charm and strange quarks and top and the bottom quarks. The quarks also come in three different colors and combine to form a colorless object. The three generations of the leptons are electron, muon and tauon with their respective neutrinos. Electron,muon and tau particles are massive and charged, but neutrinos are almost mass-less and charge-less.

There are four fundamental forces which act in the universe. They, in the increasing order of strength, are strong, electromagnetic, weak and gravitational forces. The electromagnetic and the gravitational force have a infinite range, while the weak and strong forces are of very short range. The three fundamental forces which are weak, electromagnetic and strong are mediated by particles called gauge bosons. For the weak force, these are $W^{\pm}$ and Z bosons. For the electromagnetic force, it is photon and for the strong force these are gluons. The gravitational force is said to be carried by graviton. But it is still not detected.

The standard model (SM) is the mathematical structure which governs how the fundamental particles interact by four fundamental forces. It took the final shape around 1970 and it explains almost all experimental facts and also predicts many phenomenon. Over many experiments and over a long span of time, it has established itself as a well tested physical theory. It established that the universe is made up of few fundamental building blocks and governed by four fundamental forces. The standard Model has $SU(3)_C \bigotimes SU(2)_L \bigotimes U(1)_Y$ local symmetry which is spontaneously broken to $SU(3)_C \bigotimes U(1)_Q$. This spontaneous breaking of gauge symmetry is called Higgs mechanism. In the standard model, this mechanism is implemented through a scalar doublet. The Higgs mechanism gives masses to the W and Z gauge bosons, quarks and charged leptons. One of the consequences of the Higgs mechanism is the existence of a scalar particle, the Higgs boson. The search for this particle has been going on for decades. Until recently, it was the only missing piece of the standard model.

The Higgs boson has been searched for at e^+e^- colliders, Tevatron ($p\bar{p}$ collider) and now at Large Hadron Collider (LHC) (pp collider). In this thesis, we are looking for the production of Higgs boson at LHC. The main production mechanism [1] of the Higgs boson at the LHC is $gg \to H$. This is a one loop process and has the cross section of about 40 pb at 14 TeV center of mass energy for $m_H = 125$ GeV. The next important production method is vector boson fusion, $qq' \to q''q'''H$. Here typical cross section is about 4.5 pb. The third important mechanism is the production in association with a W/Z boson. Here typical cross sections are about 2.0 pb. All these mechanisms give viable signatures of the Higgs boson production. In this thesis, we have considered another important production mechanism $pp \to t\bar{t}H$. The main decay modes [1] of the Higgs boson of mass 125 GeV are $H \to b\bar{b}, \tau\tau, WW^*$ and ZZ^*. To suppress the backgrounds, the rare decay mode $\gamma\gamma$ is also sometimes useful.

In the run I of LHC, strong evidence for a Higgs boson like particle have been seen by both CMS [2] and ATLAS [3] collaborations. In run I, the center of mass energy was 7 and 8 TeV. Both the collaborations looked for the signature through the production $gg \to H$ and subsequent decay into photons and ZZ^*. The decay modes $H \to \tau\tau$ and $H \to WW^*$ have also been investigated. On the basis of combining the results, for these decay modes, the collaborations achieved a significance of more than 5 for the signature of the Higgs boson. The collaborations announced the discovery of a Higgs boson like particle on July 4^{th}, 2012. Since then, the evidence for the SM Higgs boson has only become stronger. We have considered the channel where the Higgs boson is produced in association with a top quark pair by quark-quark or gluon-gluon annihilation. To control the backgrounds we have considered semi-leptonic decay modes of top quarks, while the Higgs boson decays into a pair of tau leptons or a pair of W bosons. When a tau lepton decays into hadrons, it will manifest itself as a tau jet. Tau jets are narrow and have few particles. This can be used to tag a tau jet. The decay of a top quark gives rise to a bottom jet. It can also be tagged. Tagging of a tau and a bottom jet play an important role in reducing the backgrounds. The typical cross section for $pp \to t\bar{t}H$ process is about 500 fb for m_H= 125 GeV. The branching ratio for the Higgs boson decaying into a tau lepton pair is 5% -8% for m_H=120-130 GeV, while it is 14%-30 % for decaying into a W boson pair.

In the first paper [4] we considered 3-4 electrons/muons + jets signature of the $pp \to t\bar{t}H$ process. In the second paper [5], we considered two leptons + jets signature. In both the cases, it was important to tag enough number of tau/bottom jets for the signal to be visible. We used ALPGEN and PYTHIA to do the calculations. We also used Madgraph sometimes.

In the first paper, we have considered five signatures. The signatures are ”4 electrons/muons”, “3 electrons/muons + a jet”, “3 electrons/muons + a tau jet”, “3 electrons/muons + a bottom jet” and “3 electrons/muons”. These signatures have two types of backgrounds from the other standard model processes: a) direct backgrounds b) mimic backgrounds. In the case of mimic backgrounds, a light quark or a gluon jet fakes a bottom or a tau jet. We considered both types of backgrounds. We looked for the viability of the signatures of a Higgs boson of mass 120, 125, 130 GeV. We applied generic kinematic cut. For the bottom jets identification and rejection rates, we took the values as 55% and 1%. For the tau jet case, we consider possibilities of low tau tagging (LTT) and high tau tagging (HTT) rates. In LTT we have taken the low value of tau jet identification, 30%, and low mimic rate 0.25%. In the case of HTT, we have high identification rate, 50%, and higher mimic rate of 1%. We also used an area variable to identify a tau jet. We found that the best four-lepton signature was “four electrons/muons + a bottom jet”. In the case of three lepton signature, the best signature is found to be “three electrons/muons + a tau jet + a bottom jet”. Both of these signatures have the significance of more than 5, with the 100 fb^{-1} integrated luminosity at 14 TeV center of mass energy at

LHC. So in the run II, these signatures may be visible within a year of the run. There are other viable signatures with three leptons that were also discussed.

In the second paper, we have considered dilepton signatures of the process $pp \to t\bar{t}H$. In particular we examined the signatures "2 electrons/muons + a tau jet + a bottom jet"($e\mu\tau b$), "2 electrons/muons + two tau jets", "2 electrons/muons + a tau jet + 2 bottom jets", and "2 electrons/muons + bottom jet + 2 tau jets". Like the first paper, we considered both direct and mimic backgrounds. We also considered two possibilities of tau tagging, LTT and HTT. Now the signatures have fewer leptons, so the backgrounds are larger. In particular, there can be large backgrounds from the $t\bar{t}$ + jets and Z + jets production. We found that these backgrounds can be managed if we identify at least two tau jets or look at the same sign lepton signature. Most promising dilepton signature were "2 electrons/muons + a tau jet + a bottom jet" with same sign leptons and "2 electrons /muons + 2 tau jets". Both of these signatures will be observable within a year of restart of LHC.

In summary, we found that tau-jet tagging is important to identify the Higgs boson through the process $pp \to t\bar{t}H$. It is specially important for the case of dilepton and trilepton signatures.

Bibliography

[1] The Anatomy of Electro-Weak Symmetry Breaking
Tome I: The Higgs boson in the Standard Model, Abdelhak Djouadi, [arXiv:hep-ph/0503172v2].

[2] Observation of a new boson at a mass of 125 GeV with the CMS experiment at the LHC, The CMS Collaboration, Phys. Lett., **B 716**, 30 (2012).

[3] Observation of a new particle in the search for the Standard Model Higgs boson with the ATLAS detector at the LHC, The ATLAS Collaboration, Phys.Lett., **B 716**, 1 (2012).

[4] Multilepton Signatures of the Higgs Boson through its Production in Association with a Top-quark Pair, Pankaj Agrawal, Somnath Bandyopadhyay, Siba Prasad Das, Physical Review, **D 88**, 093008 (2013).

[5] Dilepton Signatures of the Higgs Boson with Tau-jet Tagging, Pankaj Agrawal, Somnath Bandyopadhyay, Siba Prasad Das, [arXiv:1308.6511 [hep-ph]].

List of Publications on Which This Thesis is Based

1. Pankaj Agrawal, *Somnath Bandyopadhyay*, Siba Prasad Das, Multilepton Signatures of the Higgs Boson through its Production in Association with a Top-quark Pair, Physical Review, **D 88** , 093008 (2013).

2. Pankaj Agrawal, *Somnath Bandyopadhyay*, Siba Prasad Das, Dilepton Signatures of the Higgs Boson with Tau-jet Tagging, [arXiv:1308.6511 [hep-ph]].

List of Figures

List of Tables

Chapter 1

Introduction

The standard model (SM) has been enormously successful [1, 2, 3, 4]. Until recently, one important ingredient of the model, the Higgs mechanism, had no direct experimental support. This symmetry breaking mechanism is now called Brout-Englert-Higgs (BEH) mechanism [5, 6, 7]. The implementation of the BEH mechanism through a set of scalar fields has been a standard paradigm, which is also used in a variety of the extensions of the standard model to break the gauge symmetries and bring it to the level of the SM. One consequence of the BEH mechanism is the existence of scalar particles. The number and nature of the particles depend on the symmetry that has been broken.

In the SM, the mechanism gives rise to a neutral scalar particle – the Higgs boson. On July 4, 2012, the CMS and ATLAS collaborations at the Large Hadron Collider (LHC) announced the discovery of a boson, which appeared to be like the SM Higgs boson [1, 2]. Combining the signal of the boson from its various decay modes, more than 5 σ enhancement above the background was seen by both collaborations.

There are many important production mechanisms for the Higgs boson, like gluon fusion, W-fusion, associated production with a vector boson and the production in association with a bottom-quark pair or top-quark pair [8]. Because of the large cross-section gluon fusion mechanism was the discovery mechanism. For a 125 GeV Higgs boson, there are a number of important decay channels – $H \to b\bar{b}$, WW^*, ZZ^* and $\tau\tau$ [8]. All these major production and decay channels, including rare decays like $H \to \gamma\gamma$ have been looked for at the LHC. At the conclusion of the the run I (2009-12) of the LHC, with about 25 fb^{-1} of data at the center of mass energy of 7 TeV and 8 TeV, it has been established that this boson was indeed the long sought standard model Higgs boson. Some of its properties like spin and mass have also been measured by the CMS and ATLAS collaborations. Its mass is around 125 GeV and spin-parity is 0^+.

One of the main goals of the run II of the LHC (2015-18) would be to measure various properties of the Higgs boson, in particular its couplings to the other standard model particles. One would also like to more firmly establish that this particle is indeed a SM particle, and does not belong to its extensions or modifications. So, it would be important to identify the Higgs boson through multiple production mechanisms and decay channels. There are many important production mechanisms, like associated production with a vector boson and the production in association with a bottom-quark pair or top-quark pair which are still to be seen. Some other rare decays of the Higgs boson like $H \to Z\gamma$ will also be looked for.

The Large Hadron Collider (LHC) has completed its run I. It is getting ready for run II with upgraded C.M. energy and higher luminosity. During run I, as discussed above, a long awaited discovery was made. A long wait of 45 years was over, and the Higgs boson was discovered. With its discovery, the final missing piece of the standard model was found. We now know how quarks, leptons, W and Z bosons acquire masses. More discoveries may be in store in run II.

The first signature of the Higgs boson appeared in its production through gluon fusion and decay into a pair of photons or Z-boson (to four leptons). With the discovery, next goal is to detect Higgs boson through its various production mechanisms and multiple decay modes. The Higgs boson decay modes of a tau-lepton pair and a W-boson pair have also been seen. Goal now is to measure properties of the Higgs boson and establish beyond any reasonable doubt that it is the standard model Higgs boson.

In this thesis, we focus on the Higgs boson production in association with a pair top-quark i.e. $pp \to t\bar{t}H$. In particular we focus on the decay modes $H \to \tau\tau/WW^*$ [9, 10, 11, 12, 13]. We analyze di-lepton, tri-lepton and four-lepton signatures and show how they can be useful. The plan of this thesis is as follows. In this chapter, we give an introduction to the standard model. In the next chapter, we discuss various production mechanisms, decay modes and consequent possible signatures of the Higgs boson. In the chapter 3, we describe the initial discovery of the Higgs boson, as announced by the CMS and the ATLAS collaborations. In the chapters 4 and 5, we describe our work on the $pp \to t\bar{t}H$ production mechanism. In the last chapter, we give a summary.

1.1 The Electroweak Model

In particle physics, we deal with the constituents of matter and their interactions. Quarks and leptons are the constituents of matter and they interact via mediation of vector bosons. In this section we will discuss the electroweak component of the standard model. In this model the Lagrangian has $SU_L(2) \times U_Y(1)$ gauge symmetry which is spontaneously broken to $U_Q(1)$ gauge symmetry. We now briefly describe how this model came to be.

1.1.1 Weak Interaction Before Gauge Theory

The theory of weak interactions started as a Fermi theory of beta decay. It settled into V-A theory. An intermediate vector boson was introduced to overcome the problems of V-A theory. To solve renormalization problem of intermediate vector boson theory, BEH mechanism was used by Weinberg and Salam to construct the modern electroweak theory [5, 6, 7, 14, 15].

The Four-Fermion Theory

In 1930, Pauli proposed a light, neutral and feebly interacting particle in β decay [16]. He called it neutrino, "a neutral one". Soon after that Fermi proposed the theory of β decay, i.e $n \to p\, e\, \bar{\nu}_e$ [17]. The Fermi Lagrangian was

$$\mathcal{L}_F(x) = -\frac{G_F}{\sqrt{2}}[\bar{p}(x)\gamma_\mu n(x)][\bar{e}(x)\gamma^\mu \nu(x)] + \text{h.c.}, \tag{1.1}$$

here and below h.c. stands for hermitian conjugate.

In next few years, many β-decay like processes were discovered. They had a long life time as compared to other decays. Thus the concept of weak interaction evolved. It was found that the parity was not conserved in weak interaction [18]. It gave rise to V-A (Vector-Axial Vector) theory. The Lagrangian became

$$\mathcal{L}_{eff} = -\Big[\frac{G_F}{\sqrt{2}} J_\mu^\dagger(x) J^\mu(x)\Big] + \text{h.c.}, \tag{1.2}$$

where J_μ is the V-A (Vector-Axial Vector) weak current [19, 20]. It can be separated into leptonic and the hadronic weak currents. The expression is

$$J_\mu(x) = J_{l\mu}(x) + J_{h\mu}(x). \tag{1.3}$$

For first two generations, the leptonic current can be directly written in terms of lepton fields

$$J_l^\mu(x) = \bar{\nu}_e\gamma^\mu(1-\gamma_5)e + \bar{\nu}_\mu\gamma^\mu(1-\gamma_5)\mu, \tag{1.4}$$

and the hadronic current can be written in terms of quark fields as

$$J_h^\mu(x) = \bar{u}\gamma^\mu(1-\gamma_5)d_\theta + \bar{c}\gamma^\mu(1-\gamma_5)s_\theta, \tag{1.5}$$

where c field was introduced at that time as undiscovered charm quark. Here,

$$d_\theta = cos\theta_c d + sin\theta_c s,$$
$$s_\theta = cos\theta_c s - sin\theta_c d,$$

where θ_c is the Cabibbo angle [21].

The charm quark was introduced to solve the neutral-current problem The property of the weak interaction was the existence of a charged current with no neutral current in the lowest order. Currents are bilinear in fields and involve helicity projection operator $(1-\gamma_5)$ i.e. only left handed fermions take part in weak interaction. Thus

$$\bar{\psi}\gamma^{\mu}(1-\gamma_5)\psi = 2\bar{\psi}_L\gamma^{\mu}\psi_L. \tag{1.6}$$

Now, if we take account of only the first order in G_F, then the low energy experimental data collected over the years can be described by the V-A Lagrangian. There are some exceptions also. The non-leptonic decays like decay of B-mesons may not be correctly described by a current of type $J_{h\mu}j_h^{\mu}$, which describes effective Lagrangian as in equation no. (1.2). This happens because it does not include the strong interactions. It was also not possible to incorporate the phenomena of CP violation [22]. The V-A theory, in lowest order, was able to describe the weak interaction of elementary particle. But the Lagrangian in equation (1.2) is not sufficient for two more reasons. Firstly, it is a non-renormalizable theory and secondly it violates unitarity.

The Lagrangian (1.2) is not renormalizable, since the coupling constant G_F has a dimension of $mass^{-2}$. It implies that the higher order contributions are divergent. If we consider the coupling constant to be a small number then also the higher order terms may be large. Even if we restrict to Born approximation, still there are certain processes which violate unitarity. For example, if we consider the process $\nu_\mu e \rightarrow \mu\nu_e$ which is described by the Lagrangian in equation (1.2) then the amplitude has only J=1 partial wave and the high energy cross-section is equal to $\sigma \sim G_f^2 s$, where $s = 2m_e E$ with E being the energy of the muon neutrino in laboratory frame. But the condition of unitarity demands that the the $\sigma(J=1)$ should be bounded by s^{-1}. The above explanation says that for the energy above $\sqrt{s} \sim G_F^{-1/2} \approx 300$ GeV the theoretical cross-section which is calculated by equation (1.2) would violate unitarity.

Intermediate Vector Boson Theory

The weak current transforms like a four vector under Lorentz transformation. In analogy with QED, we can introduce a new quantum field W_μ and thus the basic interaction turned into

$$\mathcal{L}_{IVB} = g(J_\mu W^{\mu} + h.c.). \tag{1.7}$$

The four-fermion Lagrangian can be obtained from the above equation. It can be considered as a low energy interaction of four fermions from $\mathcal{L}_{IVB}$ in the second order. The Lagrangian has a term $g^2 M_W^{-2} = 2^{-1/2} G_F$. As we know that the quantum electrodynamics is a abelian gauge theory. The above Lagrangian can be considered as part of a Lagrangian of Yang-Mills theory, but it has a massive gauge boson and hence it will not preserve the unitarity and the renormalizablity of the Lagrangian.

1.1.2 Construction of the SU(2)×U(1) Theory

The mediator particle in weak interaction are $W^{\pm}$ and Z bosons. In the theory of weak interaction, the masses of the gauge bosons should be incorporated in gauge invariant way. But it turns out that when we put the mass term of $W^{\pm}$ and the Z boson, the gauge symmetry is broken. The solution was given by a mechanism called "BEH Mechanism" [5, 6, 7], in which the symmetry is spontaneously broken without spoiling the symmetry of the Lagrangian. The problem of unitarity and the renormalization are also taken care, and a unity of weak interaction and electromagnetism also appears in the theory. The required gauge symmetry is $SU_L(2) \times U_Y(1)$.

The first attempt to unify weak and electromagnetic theory was proposed by Schwinger after seeing the vector nature of both the forces [23]. Later, a Schwinger's student, Glashow, to unify the weak and the electro-magnetic theory, proposed a model which had $SU(2) \times U(1)$ gauge symmetry but renormalization was not there in the theory [24]. The solution was the BEH mechanism. The BEH mechanism as a solution was proposed first by Weinberg and later by Salam. In early 1975 't Hooft transformed the subject by proving the gauge theory is renormalizable with and without spontaneous symmetry breaking [25], thus making the Glashow-Weinberg-Salam electroweak model complete.

1.1.3 Lagrangian of the Electroweak Model

We can divide the Lagrangian of the electroweak model in four different parts.

1. The first part of the Lagrangian describes the gauge bosons

$$\mathcal{L}_1 = -\frac{1}{4}\vec{W}_{\mu\nu}.\vec{W}^{\mu\nu} - \frac{1}{4}B_{\mu\nu}B^{\mu\nu}. \tag{1.8}$$

The above piece of the Lagrangian gives the kinetic energy and the self interacting term for $W^{\pm}$, Z, γ. It contains two pieces. In the first piece we have

$$\vec{W}_{\mu\nu} = \partial_\mu \vec{W}_\nu - \partial_\nu \vec{W}_\mu - g\vec{W}_\mu \times \vec{W}_\nu. \tag{1.9}$$

Here $\vec{W}_\mu$ transforms as

$$\vec{W}_\mu \to \vec{W}_\mu - \frac{1}{g}\partial_\mu \vec{\alpha} - \vec{\alpha} \times \vec{W}_\mu. \tag{1.10}$$

In the second piece

$$B_{\mu\nu} = \partial_\mu B_\nu - \partial_\nu B_\mu. \tag{1.11}$$

The B_μ is the gauge field corresponding to $U_Y(1)$ symmetry.

2. Leptons and quarks kinetic energies and their interaction with $W^{\pm}$,Z,γ are given by

$$\mathcal{L}_2 = \bar{L}\gamma^\mu(i\partial_\mu - g\frac{1}{2}\vec{\tau}.\vec{W}_\mu - g'\frac{Y}{2}B_\mu)L + \bar{R}\gamma^\mu(i\partial_\mu - g'\frac{Y}{2}B_\mu)R. \tag{1.12}$$

The above piece of the Lagrangian gives the kinetic energy of quarks and leptons and their interaction with $W^{\pm}$, Z, γ. It contains two pieces. Here L denotes the left-handed fermion doublet and R denotes a right-handed fermion singlet. For one generation, they corresponds to $\begin{pmatrix} \nu_e \\ e \end{pmatrix}$, and e_R respectively. There is an implicit sum over generations.

The first piece of $\mathcal{L}_2$ gives the kinetic energies of all the left-handed particles which include all the three generations of leptons and quarks. The second and third terms of the first piece give the interaction of all left-handed leptons and quarks with W and B fields. The second piece of $\mathcal{L}_2$, which is $\bar{R}\gamma^\mu(i\partial_\mu - g'\frac{Y}{2}B_\mu)R$, also gives the kinetic energies of all the right-handed particles i.e. all the quarks and leptons excluding the neutrinos, as the neutrinos are left-handed particles. Right-handed singlets do not interact with W fields. With the discovery of neutrino oscillations, we know now that neutrinos have mass. However, it is not certain yet how to incorporate this mass in the electroweak model. There are many ways to do it. Since this issue does not impact our work, we will not discuss it further.

3. $W^{\pm}$, Z, γ and Higgs boson masses and the couplings are given by

$$\mathcal{L}_3 = |(i\partial_\mu - g\frac{1}{2}\vec{\tau}.\vec{W}_\mu - g'\frac{Y}{2}B_\mu)\phi|^2 - V(\phi), \tag{1.13}$$

where $V(\phi) = \mu^2\phi^\dagger\phi + \lambda(\phi^\dagger\phi)^2$.

The above piece of the Lagrangian gives the masses to the Higgs boson, $W^{\pm}$ and Z bosons and determines their couplings. It contains two pieces.

The first term of the first piece of $\mathcal{L}_3$ gives the Higgs boson kinetic energy term. The next two terms generate the masses of $W^{\pm}$ and Z bosons. This can be realized by considering these two terms. We also choose a specific vacuum to break the $SU_L(2) \times U_Y(1)$ gauge symmetries to $U_Q(1)$ symmetry. Let us consider,

$$\left|(-ig\frac{\vec{\tau}}{2}.\vec{W}_\mu - i\frac{g'}{2}B_\mu)\phi\right|^2. \tag{1.14}$$

Here the first term is

$$\begin{pmatrix} gW^3_\mu & g(W^1_\mu - iW^2_\mu) \\ g(W^1_\mu + iW^2_\mu) & -gW^3_\mu \end{pmatrix}, \tag{1.15}$$

while the second term is

$$\begin{pmatrix} g'B_\mu & 0 \\ 0 & -g'B_\mu \end{pmatrix}. \tag{1.16}$$

To break the symmetry, we expand ϕ fields around the vacuum v, where v is the vacuum expectation value of ϕ field,

$$\begin{pmatrix} 0 \\ v \end{pmatrix}. \tag{1.17}$$

The above equations when plugged in equation (1.14) give

$$(\frac{1}{2}vg)^2 W_\mu^+ W^{-\mu} + \frac{1}{8}v^2(W_\mu^3, B_\mu)\begin{pmatrix} g^2 & -gg' \\ -gg' & g'^2 \end{pmatrix}\begin{pmatrix} W^{3\mu} \\ B^\mu \end{pmatrix}, \tag{1.18}$$

where $W^\pm = (W^1 \mp iW^2)/\sqrt{2}$. We see that a mass term for the W boson has been generated with $M_W = \frac{1}{2}gv$. We can redefine the fields to diagonalize the second term. We can write this term as

$$\begin{aligned} & \frac{1}{8}v^2[g^2(W_\mu^3)^2 - 2gg'W_\mu^3 B^\mu + g'^2(B_\mu)^2], \\ = & \frac{1}{8}v^2[gW_\mu^3 - g'^2(B_\mu)]^2, \\ = & \frac{1}{2}M_Z^2 Z_\mu^2 + \frac{1}{2}M_A^2 A_\mu^2, \end{aligned} \tag{1.19}$$

where we have introduced fields

$$A_\mu = \frac{g'W_\mu^3 + gB_\mu}{\sqrt{g^2 + g'^2}} \tag{1.20}$$

and

$$Z_\mu = \frac{gW_\mu^3 - g'B_\mu}{\sqrt{g^2 + g'^2}}. \tag{1.21}$$

Clearly $m_A = 0$ and $m_Z = \frac{1}{2}v\sqrt{g^2 + g'^2}$.

4. Fourth part of the Lagrangian gives masses of quarks and leptons and their couplings to the Higgs boson. Considering, first generation of the leptons only,

$$\mathcal{L}_4^l = -y_e\Big[(\bar{\nu}, \bar{e})_L \begin{pmatrix} \phi^+ \\ \phi^0 \end{pmatrix} e_R + \bar{e}_R(\phi^-, \bar{\phi}^0)\begin{pmatrix} \nu_e \\ e \end{pmatrix}_L + \text{h.c.}\Big]. \tag{1.22}$$

We now substitute

$$\phi = \sqrt{\frac{1}{2}} \begin{pmatrix} 0 \\ v + H(x) \end{pmatrix}. \tag{1.23}$$

This substitution will break the the symmetry spontaneously and the Lagrangian becomes

$$\mathcal{L}_4^l = -\frac{y_e}{\sqrt{2}} v(\bar{e}_L e_R + \bar{e}_R e_L) - \frac{y_e}{\sqrt{2}} (\bar{e}_L e_R + \bar{e}_R e_L) H. \tag{1.24}$$

Now we can choose y_e such that $m_e = \frac{y_e}{\sqrt{2}} v$ which generates the electron mass. However neutrinos remain massless.

The above choice generates the electron mass. Thus the Lagrangian is given by,

$$\mathcal{L}_4^l = -m_e \bar{e} e - \frac{m_e}{v} \bar{e} e H. \tag{1.25}$$

Since the mass of electron is dependent upon the arbitrary coupling constant y_e, the theory doesn't give the mass of an electron. Moreover since the value of v is 246 GeV hence the coupling factor m_e/v is very small. So only couplings of the Higgs boson to heavy fermions is important.

The masses of quarks are also generated in the similar fashion as for the lepton masses. Only difference is that in order to generate the mass for the upper member of a quark doublet, we need to construct

$$\phi_c = -i\tau_2 \phi^* = \begin{pmatrix} -\bar{\phi}^0 \\ \phi^- \end{pmatrix} \xrightarrow{\text{SSB}} \sqrt{\frac{1}{2}} \begin{pmatrix} v + H \\ 0 \end{pmatrix}. \tag{1.26}$$

Here SSB stands for spontaneous symmetry breaking. The above constructed Higgs doublet has weak hypercharge opposite to ϕ which is $Y = -1$. It transform in the same way as ϕ changes and can be employed to construct a gauge invariant theory.

$$\mathcal{L}_4^{ud} = -y_d (\bar{u}, \bar{d})_L \begin{pmatrix} \phi^+ \\ \phi^0 \end{pmatrix} d_R - y_u (\bar{u}, \bar{d})_L \begin{pmatrix} -\bar{\phi}^0 \\ \phi^- \end{pmatrix} u_R + \text{h.c.} \tag{1.27}$$

$$\xrightarrow{\text{SSB}} -m_d d\bar{d} - m_u u\bar{u} - \frac{m_d}{v} \bar{d} d H - \frac{m_u}{v} \bar{u} u H. \tag{1.28}$$

In the above equation, we have taken care of only the first doublet of quarks. The weak interaction acts on $(u, d')_L$, $(c, s')_L$ and $(t, b')_L$ pairs. Here the prime states are the linear combination of flavor eigenstates. Thus the quark Lagrangian looks like,

$$\begin{aligned} \mathcal{L}_4^q \;&=\; -y_d^{ij} (\bar{u}_i, \bar{d'}_i)_L \begin{pmatrix} \phi^+ \\ \phi^0 \end{pmatrix} d_{jR} - y_u^{ij} (\bar{u}_i, \bar{d'}_i)_L \begin{pmatrix} -\bar{\phi}^0 \\ \phi^- \end{pmatrix} u_{jR} \\ &+\; \text{h.c.}, \end{aligned} \tag{1.29}$$

here i and j are flavor indices and go from 1 to 3. Thus after symmetry breaking

$$\mathcal{L}_4^q = -m_d^i \bar{d}d\left(1+\frac{H}{v}\right) - m_u^i \bar{u}u\left(1+\frac{H}{v}\right). \tag{1.30}$$

In the above, we have ignored the complication of introducing the Cabibbo-Kobayashi-Maskawa matrix. Taking into consideration the above equations $\mathcal{L}_4$ in general can be written as

$$- \quad (y_d \bar{L}\phi R + y_u \bar{L}\phi_c R) + \text{h.c.}, \tag{1.31}$$

where L stands for left handed doublet of quarks and leptons and R denotes right handed fermion singlet.

From the above discussion it is clear that the masses of the fermions are dependent on the arbitrary Yukawa couplings which are not predictable. Masses are parameters of the theory. They are to be measured by experiments. The couplings of the Higgs boson are proportional to the masses of leptons and quarks, which can be verified experimentally. We note that the minimal choice of a single Higgs doublet is enough to generate the masses of gauge bosons and fermions. Let us now again consider the scalar potential

$$V(\phi) = \mu^2\phi^\dagger\phi + \lambda(\phi^\dagger\phi)^2. \tag{1.32}$$

Using (1.23), one can find that the mass of the Higgs boson is $m_H^2 = 2v^2\lambda$. Now v is a fixed quantity, so the mass of the Higgs boson depends on λ. If m_H is very large then we cannot do the perturbation theory. On the other hand if m_H is very small then the radiative corrections can remove the minimal at $v \neq 0$. This helped put a lower bound on the mass of the Higgs boson.

Putting all the terms together, the Lagrangian for the electroweak model would be

$$\begin{aligned}\mathcal{L}_{EW} = \; & - \; \frac{1}{4}\vec{W}_{\mu\nu}.\vec{W}^{\mu\nu} - \frac{1}{4}B_{\mu\nu}B^{\mu\nu} \\ & + \; \bar{L}\gamma^\mu(i\partial - \frac{1}{2}g\vec{\tau}.\vec{W}_\mu - g'\frac{Y}{2}B_\mu)L + \bar{R}\gamma^\mu(i\partial_\mu - g'\frac{Y}{2}B_\mu)R \\ & + \; \left|(i\partial_\mu - \frac{1}{2}g\vec{\tau}.\vec{W}_\mu - g'\frac{Y}{2}B_\mu)\phi\right|^2 - V(\phi) \\ & - \; (y_d\bar{L}\phi R + y_u\bar{L}\phi_c R) + \text{h.c.}\end{aligned} \tag{1.33}$$

In this Lagrangian, sum over the leptons and quarks generations is implicit. This Lagrangian completely describes the weak and electromagnetic interactions among leptons, quarks, gauge bosons and the Higgs boson.

1.2 Quantum Chromodynamics

Results of lepton-hadron scattering strongly suggested the quark-parton model to describe the Bjorken scaling. The data also gave the hint that the field theory of strong interaction must be asymptotically free and the quarks interact feebly in high energy regime or at short distances. The quarks have another quantum number called color. By the postulate that the quarks carry color, the paradoxes and anomalies which occurred in the quark model could be resolved. The theory of strong forces must be dependent on color, as only color singlet are observable in nature. It was proposed that the strong interaction can be described by the SU(3) color Yang-Mills theory [26], where the quarks of each flavor transforms like the fundamental triplet representation [27]. The theory is called quantum chromodynamics (QCD). With q_k representing the quark field and A_μ representing gluon fields, the Lagrangian is

$$\mathcal{L}_{QCD} = -\frac{1}{2}tr(G_{\mu\nu}G^{\mu\nu}) + \sum_k \bar{q}_k(i\gamma^\mu D_\mu - m_k)q_k, \tag{1.34}$$

where

$$G_{\mu\nu} = \partial_\mu A_\nu - \partial_\nu A_\mu - ig_s[A_\mu, A_\nu], \tag{1.35}$$

$$D_\mu q_k = (\partial_\mu - ig_s A_\mu)q_k, \tag{1.36}$$

$$A_\mu = \sum_{a=1}^{8} A_\mu^a \lambda^a/2, \tag{1.37}$$

where λ_as are Gell-Mann matrices which obeys SU(3) commutation relation,

$$\left[\frac{\lambda_a}{2}, \frac{\lambda_b}{2}\right] = if^{abc}\frac{\lambda_c}{2}. \tag{1.38}$$

The normalization condition is

$$tr(\lambda^a\lambda^b) = 2\delta^{ab}. \tag{1.39}$$

The QCD Lagrangian (1.34) has all the well known strong interaction symmetries. We have conservation of charge conjugation, parity and strangeness.

The QCD is asymptotically free [28, 29]. The beta function is

$$\beta_g = \mu\frac{dg_s}{d\mu} = \frac{-1}{16\pi^2}(11 - \frac{2}{3}n_i)g_s^3 = -bg_s^3. \tag{1.40}$$

We see that as long as $n_i < 17$, b>0, the coupling decreases as the scale increases. This equation can be solved to give

$$\alpha_s(Q^2) = \frac{\alpha_s(\mu^2)}{1 + 4\pi b\alpha_s(\mu^2)ln(Q^2/\mu^2)}. \tag{1.41}$$

Here $\alpha_s(\mu^2) = g_s^2/4\pi^2$. This can be simplified by introducing the parameter Λ. One can rewrite the above equation as

$$\alpha_s(Q^2) = \frac{4\pi}{(11 - \frac{2}{3}n_f)ln(Q^2/\Lambda^2)}. \tag{1.42}$$

We clearly see that as Q increases the denominator will become larger which will decrease the value of $\alpha_s(Q^2)$. So the interaction becomes weaker as the scale increases.

1.3 The Standard Model

The standard model describes the strong, weak and the electromagnetic interactions among quarks and leptons. Its Lagrangian is

$$\mathcal{L}_{SM} = \mathcal{L}_{EW} + \mathcal{L}_{QCD}, \tag{1.43}$$

$\mathcal{L}_{EW}$ and $\mathcal{L}_{QCD}$ are given by equation (1.33) and equation (1.34). This Lagrangian has $SU_C(3) \times SU_L(2) \times U_Y(1)$ gauge symmetry, which is spontaneously broken to $U_Q(1)$, using a doublet of scalar fields. The resulting theory is in very good accord with most of collider data. This model does not include neutrino masses. There are a number of puzzles which may require us to go beyond this model. All of this is beyond the scope of this work.

Bibliography

[1] G. Aad *et al.* [ATLAS Collaboration], Phys. Lett. B **716**, 1 (2012).

[2] S.Chatrchyan *et al.* [CMS Collaboration], Phys. Lett. B **716**, 30 (2012).

[3] C. Quigg, *Gauge Theories of the Strong, Weak, and Electromagnetc Interactions* (Addison–Wesley Pub. Co., Menlo Park, 1983).

[4] T.P. Cheng and L.F. Li, *Gauge Theory of Elementary Particle Physics* (Claredon Press, Oxford, 1984).

[5] F. Englert and R. Brout, Phys. Rev. Lett. **13**, 321 (1964).

[6] P. W. Higgs, Phys. Lett. **12**, 132 (1964); P. W. Higgs, Phys. Rev. Lett. **13**, 508 (1964).

[7] G.S. Guralnik, C.R. Hagen, and T. W. B. Kibble, Phys. Rev. Lett. **13**, 585 (1964).

[8] Abdelhak Djouadi, Phys. Rept. **457**, 1 (2008).

[9] See for e.g., Pankaj Agrawal, Mod. Phys. Lett. A **14**, 1479 (1999); Pankaj Agrawal, Mod. Phys. Lett. A **16**, 897 (2001).

[10] S.Chatrchyan*et al.* (CMS Collaboration), Phys. Lett. B **713**, 68 (2012).

[11] J.Baglio and A. Djouadi, arXiv:1103.6247 [hep-ph].

[12] See for e.g., CMS Collaboration,CMS-PAS-HIG-13-015.

[13] See for e.g., CMS Collaboration, JHEP **1305**, 145 (2013).

[14] S. Weinberg, Phys. Rev. Lett. **19**, 1264 (1967).

[15] A. Salam, in *"Elementary Particle Theory", The Nobel Symposium n/bo 8*, edited by N. Svartholm (Almqvist and Wiksell, Stockholm, 1968), p./, 367.

[16] W. Pauli, *Open Letter to Radioactive Persons*, 1930, for an English translation see: Physics Today **31**, 27 (1978).

[17] E. Fermi, Z. Phys. **88**, 161 (1934); E. Fermi, Nuovo Cim. **11**, 1 (1934).

[18] T.D. Lee and C.N. Yang, Phys. Rev. **108**, 1611 (1957).

[19] R.P. Feynman and M. Gell-Mann, Phys. Rev. **109**, 193 (1958).

[20] R.E. Marshak and E.C.G. Sudarshan, Phys. Rev. **109**, 1860 (1958).

[21] N. Cabibbo, Phys. Rev. Lett., **10**, 531 (1963).

[22] M. Kobayashi and T. Maskawa, Prog. Theor. Phys. **49**, 652 (1973).

[23] J. Schwinger, Ann. Phys. **2**, 407 (1957).

[24] S.L. Glashow, J. Iliopoulos, and L. Maiani, Phys. Rev. D **2**, 1285 (1970).

[25] G. 'tHooft, Nucl. Phys. B **33**, 173 (1971); *idem*, B **35**, 167 (1971).

[26] C. N. Yang and R. L. Mills, Phys. Rev. **96**, 191 (1954).

[27] H. Fritzsch, M. Gell-Mann, and H. Leutwyler, Phys. Lett. B **47**, 365 (1973).

[28] D.J. Gross and F. Wilczek, Phys. Rev. Lett. **30**, 1343 (1973).

[29] H.D. Politzer, Phys. Rev. Lett. **30**, 1346 (1973).

Chapter 2

Production Mechanisms, Decay Modes and Signatures of the Higgs Boson

Major searches for the Higgs boson have been made at e^+e^- colliders LEP1 and LEP2, $p\bar{p}$ collider, Tevatron and now at pp collider, the LHC. At LEP2, a lower bound of the order of 115 GeV was placed through the production mechanism $e^+e^- \to ZH$ [1]. In this chapter, we will discuss important Higgs boson production mechanisms at a hadron collider. After that we will discuss various decay modes of the Higgs boson. In the end, we will briefly discuss the possible signatures and their observability.

2.1 Major Higgs Boson Production Mechanisms

In this section, we will discuss the important processes for the production of the Higgs boson at the LHC ($\sqrt{s}$=14 TeV) [2]. In figure (2.1), we display cross-sections of the Higgs boson through various important production mechanisms. We then discuss various mechanisms in some details.

2.1.1 Production of the Higgs Boson via Gluon Fusion

The production mechanisms $q\bar{q} \to H$ is not very important because of the small coupling of the Higgs boson with the light quarks. Furthermore, there is a high luminosity of gluons at the LHC. Therefore the Higgs boson production mechanism $gg \to H$ has the largest cross-section. It goes from 40.25 pb to 35.04 pb for the Higgs boson of mass range between 120 GeV to

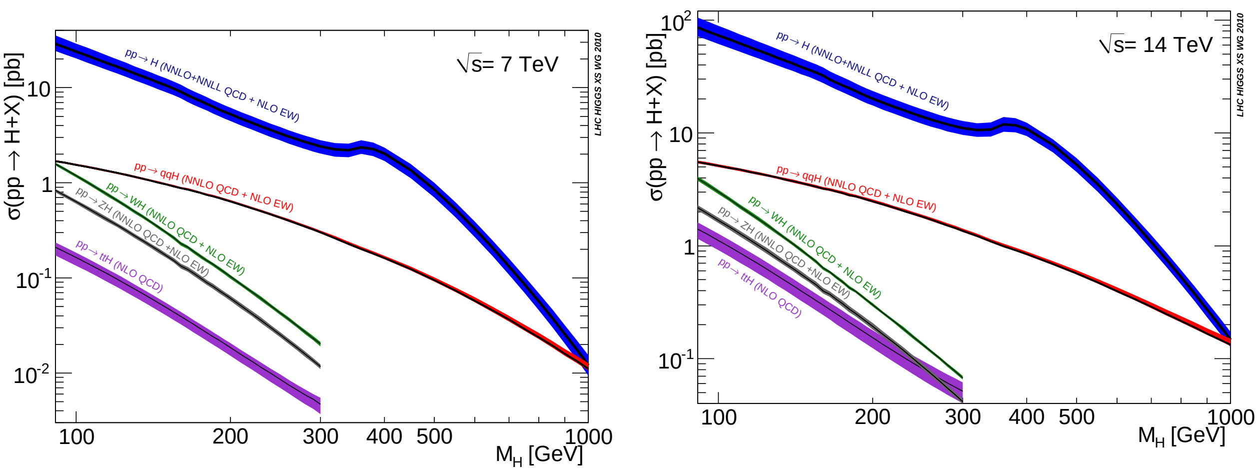

Figure 2.1: Total cross-section of the production of the Higgs boson through various processes at the CM energy of 7 TeV and 14 TeV

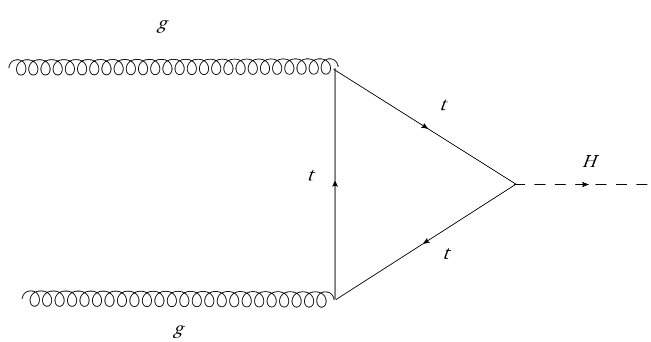

Figure 2.2: Production of the Higgs boson via Gluon Fusion

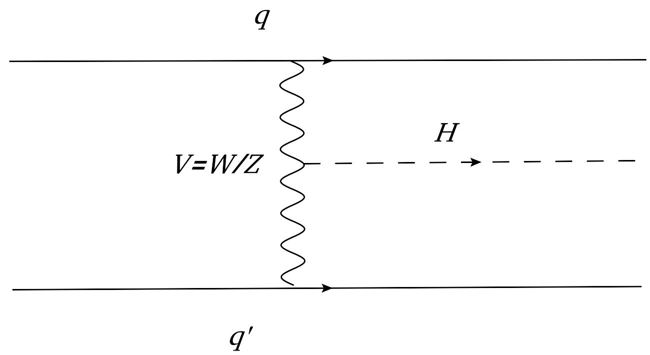

Figure 2.3: Production of the Higgs boson via Weak Vector boson Fusion

130 GeV [3, 4, 5]. The QCD radiative corrections have been studied in details to obtain the accurate theoretical predictions [6, 7, 8, 9]. We know that in QCD perturbation theory, in the lowest level loop diagrams in gluon fusion, cross-section is proportional to α_s^2, where α_s is the QCD coupling constant. The main contribution comes from the large Yukawa coupling of the top quark. The gluon coupling to the Higgs boson in the standard model is mediated by triangular loops of top quarks. Although in principle all quarks should be included in the loop, in practice the restriction to just the top quark suffices because the Higgs boson couples about 35 times more strongly to the top quark than to the next-heaviest fermion, the bottom quark, leading to a relative suppression of the bottom contribution by a factor 35^2. The next to leading order (NLO) QCD radiative corrections [6, 7, 8, 9] have been calculated in the large m_t limit and maintaining full top and bottom quark mass dependence. The NNLO cross-section calculations increase the cross-sections by 80% to about 100% at the LHC. The approximations of the large m_t is justified at the NLO. When exact Born cross-section with the full mass dependence on the top quark is used to normalize the result, the difference between the exact and the approximated NLO cross sections is very small. When the NNLO calculations are done in the above said limit, the increase in cross-sections are about 25% only. The next-to-next-leading-order have been improved by resuming the soft gluon contribution upto NNLL. These calculations result in an increase of cross-sections by an amount of 7% to 9% for a CM energy of 7 TeV and 6% to 7% for a CM energy of 14 TeV [10].

2.1.2 Production of the Higgs Boson via Weak Vector Boson Fusion

The vector boson fusion is one of the most important mechanisms for the production of the Higgs boson. In this process the quarks radiate a virtual vector boson (V^*) which annihilate to produce the Higgs boson [11, 12, 13, 14, 15]. This process has the second largest cross-section in the mass range 120 GeV - 130 GeV, as far as all the other mechanisms are concerned [16, 17, 18]. In vector boson fusion process, the QCD NLO corrections [18, 19, 20, 21] are very small, of the $\mathcal{O} \sim 5\%$ [22] and hence theoretically under control. The vector boson fusion has an added advantage that it has a very clean signature of two energetic, strongly forward jet and a central Higgs boson. This can be used to isolate the signal from the background.

2.1.3 Production of the Higgs Boson via Higgs-Strahlung Process

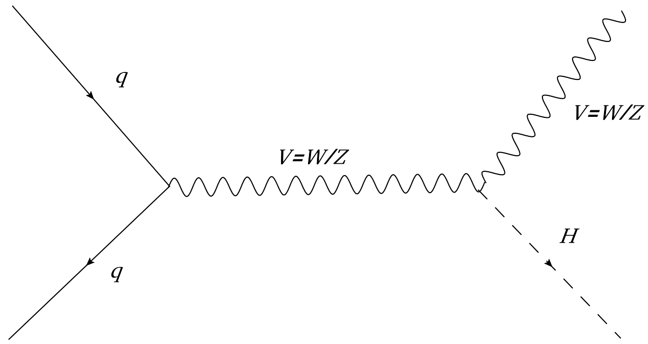

Figure 2.4: Production of the Higgs boson via Higgs-Strahlung Process

At the LHC, the cross-section of the Higgs-Strahlung process i.e. $\sigma(q\bar{q'} \rightarrow VH)$, where $V = W, Z$ boson, is not that large as compared to the two production mechanisms discussed above, over the Higgs boson in the mass range of 120 GeV - 130 GeV [23, 24]. In this process, a pair of quark, anti-quark annihilate to give a vector boson which in turn radiates a Higgs boson. Its production cross-section when it is produced in association of a W boson varies from 1.65 pb to 1.28 pb for the Higgs boson of mass 120 GeV to 130 GeV. When it is produced in association with a Z boson the production cross-section varies from 0.89 pb to 0.70 pb for the above Higgs boson mass range. If we compare $q\bar{q'} \rightarrow W^{\pm}H$ production mechanism and the production mechanism $q\bar{q} \rightarrow ZH$ cross-section, the later one is about a factor of two lower than the previous one. The QCD corrections to $\sigma(q\bar{q} \rightarrow VH)$, where V is a vector boson coincides with those of the Drell-Yan process and increase the K-factor by about 30%. The NNLO contributions [16, 17, 18, 25] increase the cross-section by 1% to 3.5% for the Higgs boson in the mass range of 120 GeV to 130 GeV.

2.1.4 Production of the Higgs Boson in Association with a Heavy Quark Pair

In the process $q\bar{q}/gg \rightarrow Ht\bar{t}$ [4, 5], the Higgs boson is radiated by a top quark. The production rate, when measured gives information about the top-Higgs Yukawa coupling. Although this process was not observable at the Tevatron, but will be a good channel at the LHC for the Higgs boson mass between 120 GeV to 130 GeV. The production cross section goes from 0.70 pb to 0.56 pb for the Higgs boson in this mass range. (When factorization and renormalization scales are set equal to $m_Q + \frac{1}{2}M_H$.) The full next-to-leading-order (NLO) calculations have been done and the increase in cross-section is about 20% of the tree level cross-section, which depends upon the mass of the Higgs boson and the parton distribution functions used in the calculations. The next-to-leading-order (NLO) calculations shows that the value of K-factor is

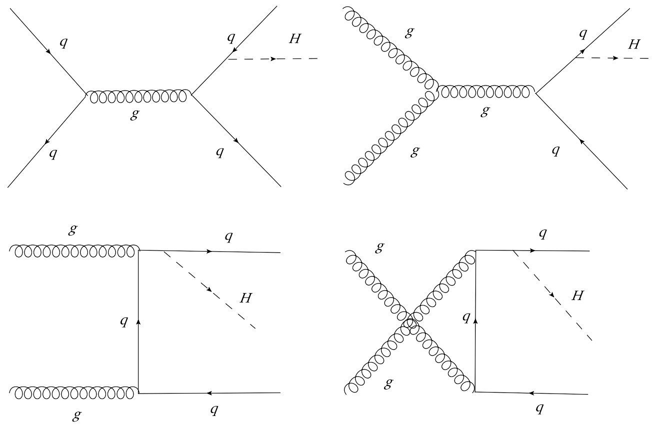

Figure 2.5: Production of the Higgs boson in Association with a Heavy Quark Pair

almost equal to 1.2 for the Higgs boson of mass range 120 GeV to 130 GeV.

The cross-section for the process $pp \to Hb\bar{b} + X$ is quiet small due to small Yukawa coupling of $Hb\bar{b}$, [26, 27] $g_{bbH} = m_b/v \sim 0.02$. The production cross section of $q\bar{q}, gg \to b\bar{b}H$ is about 5.3×10^2 fb for the Higgs boson of mass 125 GeV at the leading order. It increases to 5.8×10^2 fb when NLO corrections are included. In four-flavor scheme where there is no b quark in the initial state, the lowest order processes are $q\bar{q} \to b\bar{b}H$ and $gg \to b\bar{b}H$. The inclusive cross-section for the process $gg \to b\bar{b}H$ has large logarithms proportional to $L_b \equiv log(Q^2/m_b^2)$ which arise due to splitting of gluons into $b\bar{b}$ pairs. Since $Q \gg m_b$ the splitting is of the order of $(\alpha_s L_b)$. Because of the large logarithms, the perturbative convergence may be very poor. Summing the collinear logarithms to all orders in perturbation theory, convergence can be improved. This can be done by using b-quark parton distribution at the factorization scale $\mu_F = Q$. This calculation is governed by the fact that outgoing b-quark has a small transverse momentum. Hence the incoming b partons have been assigned a zero transverse momentum at the leading order. They acquire a transverse momentum at the higher order. The predictions of the leading order for these processes have large uncertainties. However, when higher order corrections are included these scheme and the scale dependence are significantly reduced.

2.2 Major Decay Modes

The standard model Higgs boson is heavy and can decay into many channels. The most prominent are its decay into two bottom quarks, two Ws, two tau leptons, two gluons or two charm quarks in decreasing order of their branching ratios. These decay channels are prominent in the mass range 120 GeV to 130 GeV of the Higgs boson. Apart from these modes the Higgs boson may decay with smaller branching ratios to ZZ^*, $\gamma\gamma$, $Z\gamma$, ss, $\mu\mu$ and so on.

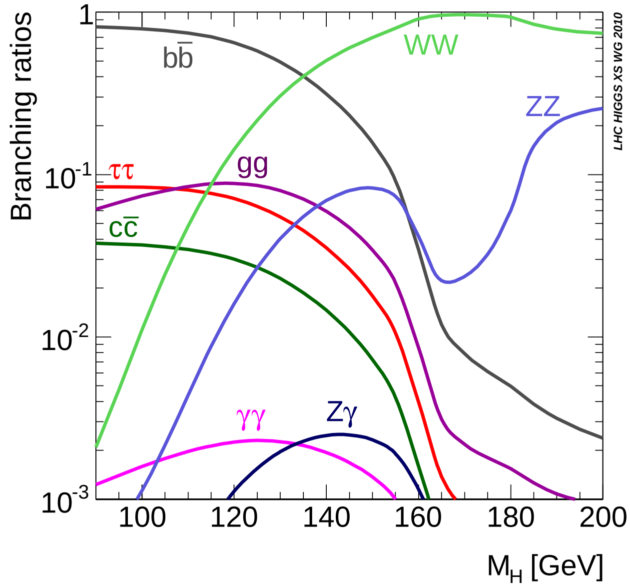

Figure 2.6: Major Decay Channels of the Higgs boson

The largest decay mode of the Higgs boson in the mass range 120 GeV to 130 GeV is $H \to b\bar{b}$. The branching ratio is very large for this decay channel and goes from 0.68 to 0.53 in this mass range. The second most important decay of the Higgs boson in this mass range is its decay into two W bosons, where the branching ratio goes from 0.13 - 0.28 in the above mass range.

The third important decay of the Higgs boson in this mass range is $H \to \tau^+\tau^-$. The decay mode $H \to \tau\tau$ is sub-dominant having a branching ratio of 6.78×10^{-2} to 5.36×10^{-2} between the mass range of 120 GeV to 130 GeV. There are at least two features of this decay mode that are in its favor: 1) the decay products are leptons, so there will be less of a strong interaction background; 2) the branching ratio is not very small, about 5% in the mass region of interest. It's this decay mode we consider.

The another decay channel through which the Higgs boson can decay is its decay into two gluons. The Branching ratio varies from 6.88×10^{-2} to 6.30×10^{-2} for the above mass range. The Higgs boson sometimes also goes to $c\bar{c}$ with branching ratio of 3.15×10^{-2} to 2.45×10^{-2} in this mass region.

Although above decay modes have large branching ratios, but there is usually a large background from QCD processes. Therefore, it is the rare decays which have played important role in the discovery of the Higgs boson. These rare decays are $H \to \gamma\gamma$ and $H \to ZZ^*$ with subsequent decays into four leptons. The background to these processes is under control. The branching ratio for $H \to \gamma\gamma$ varies from 3×10^{-3} to 2×10^{-3}, while for $H \to ZZ^*$ it goes from 3×10^{-2} to 2×10^{-2} in the mass range of 120 GeV to 130 GeV.

2.3 Signatures of the Higgs Boson

Once we know prominent production mechanisms and major decay modes, we can determine the important signatures of the Higgs boson. We will now go through different production mechanisms and discuss their useful signatures.

2.3.1 The gg $\rightarrow$ H Mechanism

The gluon fusion via a heavy quark loop is the main production mechanism of the standard model Higgs boson at the LHC. When this production mechanism is combined with the decay channels viz. $H \rightarrow \gamma\gamma$, $H \rightarrow \tau\tau$, $H \rightarrow WW^*$, $H \rightarrow ZZ^*$, we obtain some of the most promising signatures for the Higgs boson at LHC in the mass range of 120 GeV to 130 GeV.

The H $\rightarrow \gamma\gamma$ channel

For the Higgs boson between the mass range 120 GeV to 130 GeV, it has been one of the most promising detection channel [28, 29]. The loop induced process $gg \rightarrow \gamma\gamma$ contributes half the backgrounds. The direct process $q\bar{q} \rightarrow \gamma\gamma$ produces the rest of huge amount of background. A rejection factor of $\mathcal{O}(10^6)$ is needed to bring it down to the manageable order. The branching ratio of the Higgs boson is about 2.16×10^{-3} to 2.21×10^{-3} within this mass range. This is the process in which the first hint of the Higgs boson was seen at the LHC. This has been the discovery channel of standard model Higgs boson.

The H $\rightarrow WW^*$ channel

This is the second important decay mode. Here WW^* in turn goes to lepton pairs $e^{\pm}/\mu^{\pm}$ along with their neutrinos [38, 39]. Now $H \rightarrow WW^* \rightarrow \ell\ell\nu\nu$ final state is attained by only 4% of WW pair, but it gives a clean signal. Here the advantage is that the $H \rightarrow WW^*$ branching ratio is large enough. But on the other hand we cannot construct the four momentum of the neutrinos and hence the Higgs boson mass cannot be fully reconstructed. About 68% times W decay into hadrons and about 33% times it decay into leptons. Therefore one can also look at state $H \rightarrow e^{\pm}/\mu^{\pm} + 2j$. These signatures of the Higgs boson have been seen at LHC.

The H $\rightarrow ZZ^*$ channel

Two gluons when fused gives a Higgs boson which in turn can decay into two Z bosons. It is a major signature. The backgrounds are $gg, q\bar{q} \rightarrow ZZ$ processes. When Z boson decays to quarks which is about 70% of the time, the other backgrounds are $gg \rightarrow Zjj$, $gg \rightarrow WW$ and

$gg \rightarrow Wjj$ etc. as specific to case by case. However when $H \rightarrow ZZ^*$, which in turn goes to $4\ell^{\pm}$ leptons is a golden channel [24, 28, 29, 30]. It may be noted that one of the Z bosons is virtual. The branching ratio of $H \rightarrow ZZ^*$ is only 1.49% - 3.80% in the above mass range. This is the decay mode, along with $H \rightarrow \gamma\gamma$, where the Higgs boson was first seen at the LHC.

The $H \rightarrow \tau^+\tau^-$ channel

Higgs boson produced via gluon fusion can decay into two τ leptons which in turn decay into either leptons or hadrons. A tau lepton decaying into leptons is always associated with a corresponding neutrino to conserve lepton number. Therefore in this decay mode the Higgs boson mass can not be reconstructed easily. The hadronic decays of a tau lepton also has a neutrino but the tau lepton can be identified as a hard jets. These jets have a high p_T value and are narrow. They can be detected in electromagnetic calorimeter. This decay mode has been seen at the LHC recently.

2.3.2 The Vector Boson Fusion Mechanism

In this process, accompanying jets haves low p_T and are close to the beam pipe and can be tagged. The various backgrounds can be eliminated by central soft-jet vetoing and double forward jet tagging. After the proper vector boson cuts are applied, the background is still very large. The production cross-section is about few pico-barn for the Higgs boson of mass range M_H = 120 GeV - 130 GeV. The ratio of signal events to the background events is about one. However this process is a theoretically clean process as the renormalization, factorization scale dependence and PDF uncertainties are small. At the LHC, this process will play important role in determining the couplings of the Higgs boson with other standard model particles.

The H $\rightarrow \gamma\gamma$ channel

This channel will give a rather clean signature. It virtually contains very little background, but the branching ratio of the Higgs boson going into two photons is very small and hence it is a rather exotic process. The backgrounds are $pp \rightarrow jj\gamma\gamma$, $pp \rightarrow W\gamma\gamma$, $pp \rightarrow Z\gamma\gamma$, when W and Z bosons decay hadronically. With high luminosity this process may be seen at the LHC.

The H $\rightarrow b\bar{b}$ channel

If we consider the decay channel $H \rightarrow b\bar{b}$, then the signature will be 4 jets. A overwhelming QCD background is $pp \rightarrow 4j$. Because of very large background very special techniques would be needed to see this channel.

The H $\to \tau\tau$ channel

This is a very promising channel for detecting a Higgs boson between mass range 120 GeV $\leq M_H \leq$ 130 GeV. The signatures $qqH \to qq\tau\tau \to qqee/\mu\mu + \not{E}$, $qqe\mu + \not{E}$, and $qq\ell h + \not{E}$ can give a large significance, specially with τ jet tagging.

The H $\to WW^*$ channel

When a Higgs boson is formed via vector boson fusion we have two hadron jets plus a Higgs boson in the final state. When the Higgs boson decays into two W bosons the background of the above process are $pp \to jjWW$ $pp \to jjjj, pp \to jjtt$ and others, which depends on how W boson will decay.

In this process, when both of the Ws decay into leptons and their corresponding neutrinos, the Higgs boson mass cannot be reconstructed [31]. This process may not be a very good discovery channel. When W bosons will decay into hadrons/leptons, with proper cuts, the background can be removed [12, 24, 32]. In simulations, which is done at parton level the $qqH \to qq\ell\nu\ell\nu$ channel, the signal and the $t\bar{t}$ plus zero, one and two jet backgrounds has been studied. It has been found that one may be able to detect the Higgs boson through this channel.

The H $\to ZZ^*$ channel

Calculations for this channel have also been done for the LHC [33, 34]. But $H \to ZZ^*$ branching ratio is very small. Above it, the branching ratio of $ZZ \to \ell\ell\ell\ell$ is also very small and $ZZ \to \ell\ell jj$ has to be considered. The largest background for this process is $pp \to Z+4j$. There are number of other significant backgrounds to this channel. This process would be visible at very high luminosity only.

2.3.3 The Higgs Straulang Mechanism

The production of the Higgs boson in association with a vector boson, when vector boson decays into $\ell = e^\pm/\mu^\pm$ can be a good channel for the detection of the Higgs boson. This process has also been looked for at the LHC and can be seen.

In the case of $pp \to HW$, the $W \to \ell\nu$ the branching fraction is 0.2. For the $pp \to HZ$ process, $Z \to \ell\ell$ the branching fraction is 0.06. The cross-section of $qq' \to WH$ production is 1.5 times more than $qq' \to ZH$ cross-section. Hence the number of signal events for the process $pp \to HZ \to H\ell\ell$ will be much smaller. The approximate branching ratio of $Z \to \nu\bar{\nu}$ is about 18% which has also be taken into consideration in literature. Overall $pp \to HW$, will be a good process to observe.

The $H \to \gamma\gamma$ channel

When the vector boson decays hadronically and the Higgs boson decays into two photons the signature is $pp \to jj\gamma\gamma$ The major backgrounds will be direct production of $pp \to jj\gamma\gamma$. This process has been studied in literature. Because of smaller cross-section, this has limited value.

The H $\to b\bar{b}$ channel

In this channel, when W-boson decay hadronically, the QCD backgrounds cannot be controlled. Therefore, one considers the leptonic decay of W boson, When $H \to b\bar{b}$, the final state would have $e^\pm/\mu^\pm + 2j$. Even here the background from $pp \to Wjj, t\bar{t}$ will be very high. Therefore tagging of the jet as a bottom jet would be important. The signature of $e^\pm/\mu^\pm + 2b$ will be useful with proper cuts to eliminate $Wb\bar{b}$ and $t\bar{t}$ backgrounds. Observation of an extra jet which is not hard has been found to increase the viability of this signature. At the LHC, this is a very useful signature. It has already been looked for at the LHC.

The H $\to \tau\tau$ channel

In this channel the number of events are very small because the $H \to \tau\tau$ branching ratio is small, of a few percent. Here calculations are done for the signal $pp \to ZH/WH \to jj\tau\tau$. A large luminosity and improved tau identification mechanism is needed to detect the signal at the LHC [32, 35].

The H $\to WW^*$ channel

The branching ratio of $H \to WW^*$ in the mass range 120 GeV $\leq M_H \leq$ 130 GeV is very large and hence a good discovery channel [32, 36, 37]. The background is $pp \to WW + W/Z$ which is overwhelming and irreducible. The $t\bar{t}$ pair production also add considerably towards the background. Here the signature can be $pp \to HW/HZ \to WW^*jj \to \ell\ell jj, pp \to HW/HZ \to WW^*jj \to \ell\ell jj$ and $pp \to HW/HZ \to WW^*jj \to \ell\ell + \not{E}_T$. Over all this is a useful channel.

The H $\to ZZ^*$ channel

The branching ratio of $H \to ZZ^*$ is very small [33, 34] in the mass range 120 GeV $\leq M_H \leq$ 130 GeV. The cross-section for the process $pp \to HW/HZ \to ZZ^*\ell\nu/ZZ^*\ell\ell$ can be small but the process is very clean and can be seen at LHC with large luminosity.

2.3.4 The $pp \to t\bar{t}H$ Mechanism

The signatures of this process is the topic of this thesis. This process, when $H \to b\bar{b}$ has been looked for at the LHC. In this thesis, we are interested in the signatures when $H \to \tau\tau, WW^*$. With these decay modes, we can have multi-jet signatures, e/μ +jets, di-lepton + jets, and multileptons + jets signatures. First two signatures are still under study. Last two signatures have been studied and the results are reported. All these signatures can be seen at the LHC with enough luminosity. One of the measure findings is the importance of the tau-jet tagging to reduce the backgrounds. We will discuss these signatures in detail in chapters 4 and 5.

Bibliography

[1] ALEPH, DELPHI, L3, OPAL Collaborations, and LEP Working Group for Higgs Boson Searches, Phys. Lett. B **565**, 61 (2003).

[2] http://en.wikipedia.org/wiki/Higgs_Boson.

[3] Abdelhak Djouadi, Phys. Rept. **457**, 1 (2008).

[4] R. Raitio and W. W. Wada, Phys.Rev D **19**, 941 (1979).

[5] J. Ng and P. Zakarauskas, Phys. Rev. D **29**, 876 (1984).

[6] M. Spria, A Djouadi,D. Garudenz and P. M. Zerwas, Nucl. Phys.B **453**, 17 (1995).

[7] A. Djouadi, M. Spira, and P. M. Zerwas, Phys. Lett. B **264**, 350 (1992).

[8] S. Dawson, Nucl. Phys. B **359**, 283 (1991).

[9] D. Garudenz, M.Spira, and P.M. Zerwas, Phys. Rev. Lett. **70**, 1372 (1993); M. Spira, Ph.D. Thesis, RWTH Aachen,1992.

[10] Status of Higgs Boson Physics http://pdg.lbl.gov/2013/reviews/rpp2013-rev-higgs-Boson.pdf.

[11] D .R. T. Jones and S. T. Petcove, Phys. Lett. B **84**, 440 (1979).

[12] R. N. Cahn and S. Dawson, Phys. Lett. B **136**, 196 (1984) and (E) ibid. B **138**, 464 (1984).

[13] D. Dicus and S. Willenbrock, Phys. Rev. D **32**, 1642 (1985).

[14] G.Altarelli, B.Mele and F.Pitolli, Nucl. Phys. B **287**, 205 (1987).

[15] W. Kilian, M. Kramer, and P. M. Zerwas, Phys. Lett. B **373**, 135 (1996).

[16] T. Han and S. Willenbrock, Phys. Lett. B **273**, 167 (1990).

[17] H. Baer, B. Bailey, and J. Owens, Phys. Rev D **47**, 2730 (1993), J. Ohnemus and W. Stirling, Phys. Rev. D **47**, 2722 (1993); S.Mrenna and C. P. Yuan, Phys. Lett. B **416**, 200 (1998).

[18] A. Djouadi and M. Spira, Phys. Rev. D **62**, 014004 (2000).

[19] T. Han, G. Valencia and S. Willenbrock, Phys. Rev. Lett. **69**, 3274 (1992).

[20] T. Figy, C. Oleari and D. Zeppenfeld, Phys. Rev. D **68**, 073005 (2003).

[21] E.L. Berger and J.Campbell, Phys. Rev. D **70**, 073011 (2004).

[22] Paolo Bolzoni, Fabio Maltoni, Sven-Olaf Moch, Marco Zaro [arXiv:1003.4451 [hep-ph]].

[23] S. L. Glashow, D. Nanopoulus and A. Yildiz, Phys. Rev. D **18**, 1724 (1978); J. Finjord, G. Girardi and P. Sorba, Phys. Lett. B **89**, 99 (1979).

[24] D. Rainwater and D. Zeppenfeld, JHEP **9712**, 005 (1997).

[25] O. Brein, A. Djouadi, and R. Harlender, Phys Lett. B **579**, 149 (2004).

[26] R. M. Barnett, H. E. Haber and D. E. Soper, Nucl. Phys. B **306**, 697 (1988); F. I. Olness and W. K. Tung, Nucl. Phys. B **308**, 813 (1988).

[27] D. A. Dicus and S. Willenbrock, Phys. Rev. D **39**, 751 (1989).

[28] J. Gunion, P. Kalyniak, M. Soldate and P. Gallison, Phys. Rev. D **34**, 101 (1986).

[29] J. Gunion, G. Kane and J. Wudka, Phys. Lett. B **299**, 231 (1988).

[30] J. Stirling, R. Kleiss and S. D. Ellis, Phys. Lett. B **163**, 261 (1985); J. Gunion, Z. Kunast, and M. Soldate, Phys. Rev. D **34**, 826 (1986); E. Glover, J. Ohnemus and S. Willenbrock, Phys. Rev. D **37**, 3193 (1988); V. Barger, G. Bhattachrya, T. Han and B. Kniehl, Phys. Rev. D **43**, 779 (1991).

[31] D. Rainwater, D. Zeppenfeld, Phys. Rev. D **60**, 113004 (1999), and (E)ibid. D **61**, 09901 (1999).

[32] S. Asai *et al.* [ATLAS Collaboration], Eur. Phys. J. C **32S2**, 19 (2004).

[33] H. D. Yildiz, M. Zeyrek and R. Kinnunen , CMS-NOTE-2001/050.

[34] K. Cranmer, B. Mellado, W. Quayle and S. L. Wu, Note ALT-PHYS-2004-005; Michel Duhrssen, Ph.D. Thesis , [http://arxiv.org/pdf/1207.2516.pdf].

[35] M. Klute, ATLAS Note ATL PHYS-2002-018(2002) Nucl. Phys. B **169**, 352 (2007); G. Azuelos and R. Mazini, ATL-PHYS-2003-004, http://cds.cern.ch/record/685437/files/phys-2003-004.pdf.

[36] C. Buttar, K. Jacobs, and R. Harper, ATL-PHYS-2002-033; N. Akchurin *et al.*, CMS-Note-2002/016; K. Cranmer B. Melloado, W. Quayle, and S. L. Wu, ATLAS Notes ATL-PHYS-2003-007 and ATL-PHYS-2003-008. N.Akchurin *et al.*, CMS-NOTE-2002/016.

[37] M. Dittmar, Pramana **55**, 151 (2000); M. Dittmar and S. Nicollerat, CMS-Note 2001/306.

[38] M. Dittmar and H. Dreiner, Phys. Rev. D **55**, 167 (1997); M. Dittmar, [hep-ex/9901009].

[39] D.Green *et al.*, J.Phys. G **26**, 1751 (2000); K. Jakobs and Th. Trefzger, Atlas Note ALT-PHYS-2003-024.

Chapter 3

Discovery of the Higgs Boson

The Higgs boson was searched at many collider, including the LEP1, LEP2 and Tevatron. Before LHC began operation in 2009, the lower bound on the mass of the Higgs boson was of the order of 115 GeV [1]. The bound came from LEP2 where the Higgs boson could be produced through the process $e^+e^- \rightarrow ZH$ and $e^+e^- \rightarrow \nu_e\bar{\nu}_e H$. The LEP2 precision data also produced an upper bound of approximately 180 GeV [2]. There was also provisional exclusion of the mass range 160 - 166 GeV at the Tevatron [3]. These bounds overshadowed lower theoretical vacuum stability bound and upper theoretical bound based on triviality of scalar field theory [4]. At last the Higgs boson was discovered at the LHC [5]. The discovery was made using the CMS and ATLAS detectors. In 2012, the CMS and ATLAS collaborations presented strong evidence for the existence of the Higgs boson of mass about 126 GeV. Subsequent analysis of the data has confirmed the evidence for the Higgs boson. In this chapter, we will first discuss the LHC, then the CMS and the ATLAS detectors. We will also discuss how the Higgs boson was discovered.

3.1 The Large Hadron Collider (LHC)

Currently, the LHC is world's most powerful particle accelerator. It works on the principle that by continuously passing the protons through a radio frequency field one could accelerate the protons rotating in a magnetic ring to higher and higher energy indefinitely. However there is a limit to the increase in the energy. When any charged particle rotates in a magnetic ring there are synchrotron losses. The synchrotron losses of an accelerating proton is about few keV per turn at the LHC. The LHC has a high luminosity of $10^{33}\,\mathrm{cm}^{-2}\mathrm{s}^{-1}$ and a data taking efficiency equal to 10^7 seconds per year. This high luminosity is achieved by strong currents. A set of dense proton bunches containing up to 110 billion protons per bunch pass through the accelerator. The distance between the two consecutive bunches is about 25 ns, in a distance

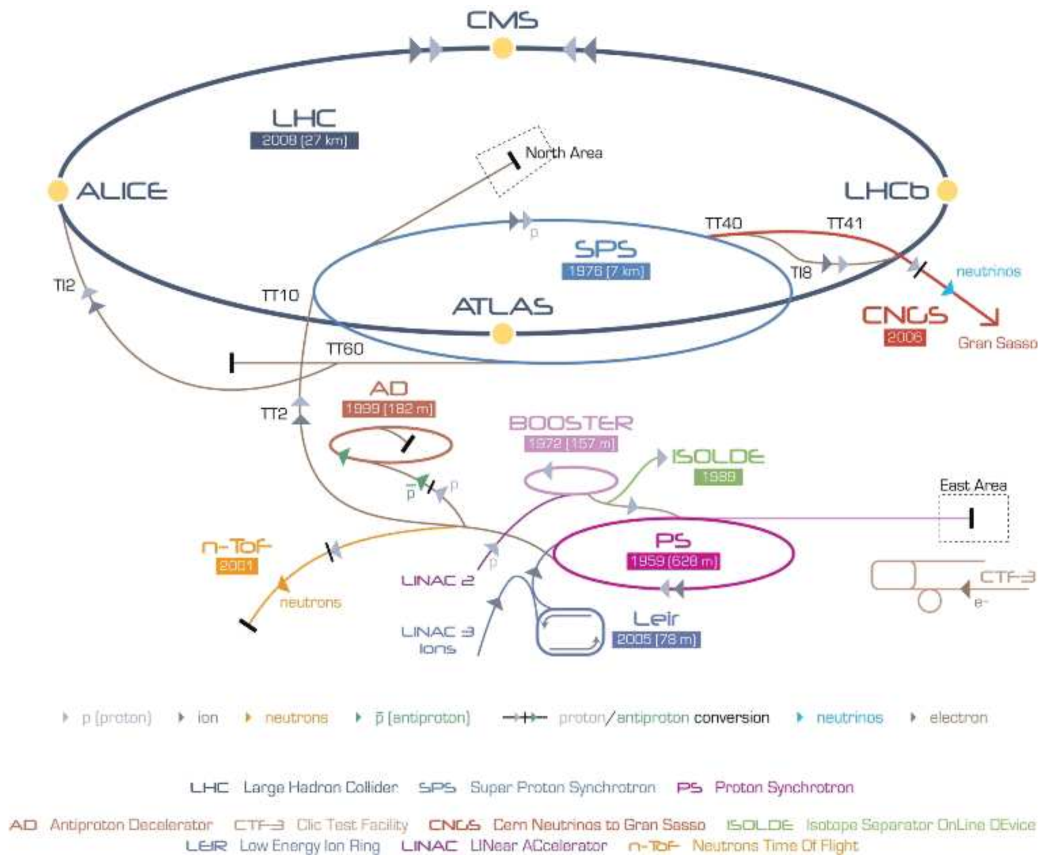

Figure 3.1: The LHC at the border of Switzerland and France with its detectors

of 7.5 m. It is also required to squeeze the protons transversely by using magnetic lenses to a small spot so that the probability of collision of two protons increases [6].

There are several steps for accelerating a proton beam in the LHC. Protons are obtained by stripping electrons from hydrogen atoms. This proton beam is accelerated by a series of accelerators. First one uses LINAC-2, which pre-accelerates the protons to 50 MeV. This is followed by Proton Synchrotron Booster (PSB). PSB consists of four superimposed rings which accelerate the protons to 1.4 GeV. Then two large circular rings further accelerate the protons to an energy of 26 GeV through Proton Synchrotron (PS) and 450 GeV through Super Proton Synchrotron (SPS). This beam is inserted into LHC. The beams are transferred from SPS to the LHC machine via 3 km long transfer line. To provide appropriate bunch distance, size and intensity the PSB-PS-SPS require significant upgradation of energy from one channel to the other.

The energy increases by a factor of 10-20 in each acceleration step. The creation of bunch pattern and the proton bunches is done by injector. The chain can be summarized as follows: 66 booster bunches are injected into the PS; each of these is split into 12 smaller bunches giving a total of 72 bunches at extraction; between 2 and 4 batches of 72 bunches are injected into the SPS giving from 144 up to 288 bunches; finally, a sequence of 12 extractions of (up to) 288 SPS bunches is injected into the LHC, giving a maximum of 2808 bunches (39 groups of 72 bunches). The filling scheme (difference between the 3564 possible and 2808 actually filled bunches) foresees a number of short gaps for, e.g., kicker magnet rise times in the injection chain.

The protons when injected to the LHC apparatus are accelerated from a range of 450 GeV to 7 TeV. This acceleration is gained in about 20 minutes. The average energy received by the protons is about 0.5 MeV per turn when passing the electrical radio-frequency (RF) fields created in 8 superconducting cavities per beam with a peak accelerating voltage of 16 MeV.

The LHC consists of arcs of 2.45 km with bending dipole magnets and 8,545 m long straight sections. The LHC has a circumference of about 27 km. The strong magnetic field of about 8.3 T is provided by super conducting electromagnets which are kept at 1.9 K. There are 1232 dipoles and 392 quadruples. The cost of the project is about 5 billion euros. The 4 major particle detectors ATLAS, CMS, ALICE and LHCb have been constructed and are placed in a huge underground caverns located at four of the straight sections. Some specialized detectors will also be used for specific purposes. These are TOTEM, LHCf and MODAL.

3.2 The ATLAS and CMS Detectors

The CMS and the ATLAS are general purpose detectors which can measure physical events of interest in the high luminosity of 7 TeV - 14 TeV pp collisions [7, 8]. The range of detector span from charm and beauty physics at lowest transverse momenta (3 GeV), to new physics searches up to the highest reachable scales (4 TeV). The cross-sections of interesting physical processes vary over many orders of magnitude at the LHC. They range from dominating QCD process to rare high scale processes. The vast scales that are to be explored at the LHC drive the detector design.

Both the ATLAS and CMS detectors have four major components:

- inner tracker
- calorimeters
- muon spectrometer
- magnet systems

Actual design and performance for these components vary for both the detectors.

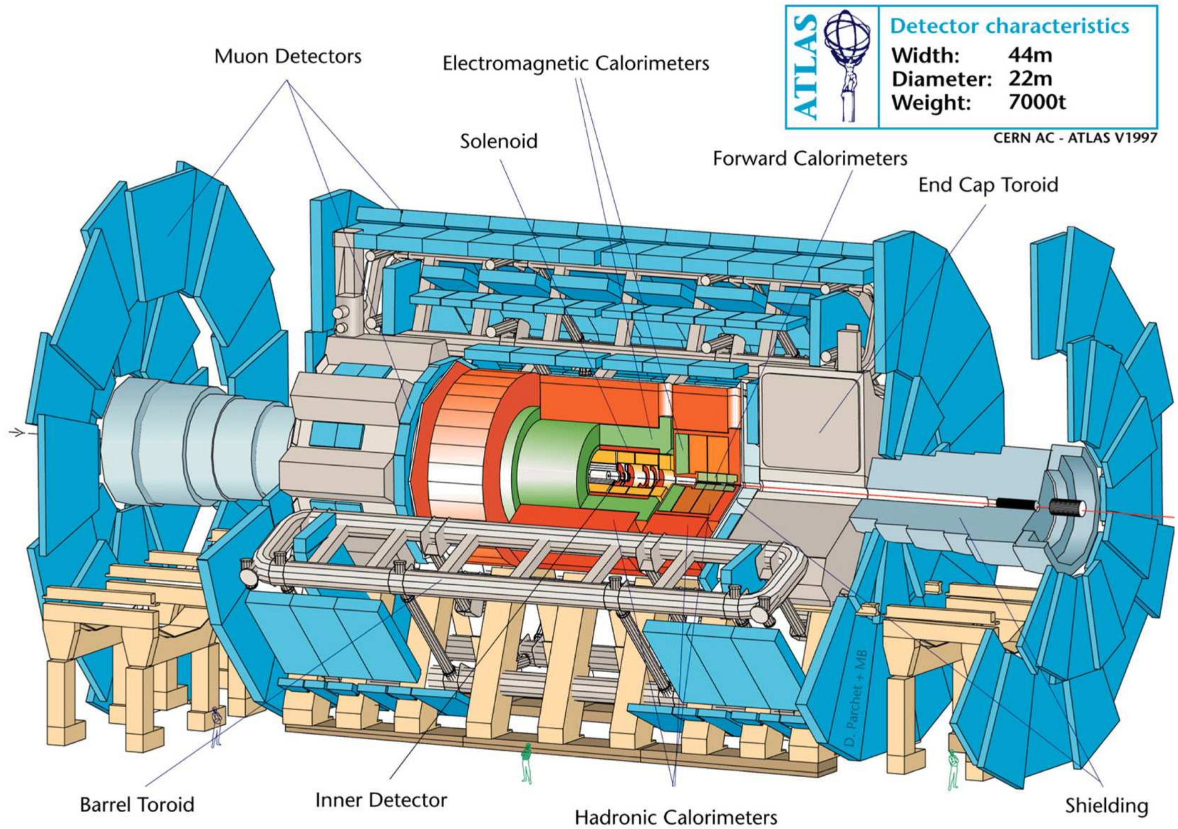

Figure 3.2: The schematic diagram of the ATLAS detector

3.2.1 The ATLAS Detector

This is a general purpose detector. Its magnet system is toroidal in shape. It is 46 m long, 25 m high and 25 m wide. It weighs 7000 tons. In run I, it collected integrated luminosity of 27.03 fb^{-1}. Its all system have been upgraded for run II that will start from April 2015. In run I, its trigger system selected about 100 interesting events per second from 500 million collision per second.

The ATLAS Inner Detector

The inner detector starts from few centimeter from the proton beam axis. It has a radius of 1.2 meters and it is about 7 meters in length [9, 10, 11]. Its function is to detect the charged particles when the particles interact with the material at the discrete points of the detector. It gives the detailed information about the type of the charged particles and about their momentum.

The Pixel detector is the innermost part of the detector which has three concentric layers of three disks on the each end-cap, with total 1,744 modules, each measuring 2 cm$\times$6 cm. The detecting material is about 250 micrometers thick silicon layer. The smallest unit which can be read out is about 50×400 micrometers. The number of pixel is about 47,000.

The middle component of the inner detector is the Semi-Conductor Tracker (SCT). It has same function as the pixel detector. It is the most critical part of the inner detector. The Semi-Conductor Tracker is used for basic tracking in the plane perpendicular to the incoming beams. It measures particles over a much larger area than the pixel detector, with equal accuracy but with more sampled points.

The Transition Radiation Tracker (TRT) is the outermost component of the inner detector. It is a combination of a transition radiation detector and straw tracker. The uncertainty of position resolution is about 200 μm. This detector is not as precise as the above discussed detectors. In TRT, particle paths with many very strong signals can be identified as belonging to the lightest charged particles i.e. electrons and positrons.

The ATLAS Calorimeters

The calorimeters are placed at the outer part of the solenoidal magnet which surrounds the inner detector [12, 13]. It measures the energy of the particles by absorbing them. The two parts of the calorimeters are inner electromagnetic calorimeter and the outer hadronic calorimeter. Here both the calorimeters are sampling calorimeters [14].

The inner electromagnetic calorimeter absorbs the energy from the charged particles as well as photons. Whereas the hadron calorimeter absorbs energy from those particles that pass from the electromagnetic calorimeter but do not interact with it. It is less precise than the inner calorimeter in terms of energy magnitude and localization.

The calorimeter consists of metal plates that acts as absorber and sensing elements. The interaction of the particles with the metal plates converts it into a ‘shower’. The showers in the Argon, liberates electron which are then recorded. In the outer section, the sensors are tiles of scintillating plastic. The showers lead the plastic to emit photons which are thus recorded.

The ATLAS Muon Spectrometer

The muon spectrometer is the one of the largest tracking system of the ATLAS [15, 16]. It consists of three parts: a magnetic field provided by 3 toroidal magnets, a set of 1200 chambers which measure the tracks of the outgoing muons, with high spatial precision and a set of triggering chambers. This sub-detector extends from a radius of 4.25 m close to the calorimeters out to the full radius of the detector i.e. 11 m. The large size of muon spectrometer is used to measure the momentum of the muons accurately. The detector is tuned to measure the momentum of 1 TeV muons with 10% accuracy and momentum of 100 GeV muons with 3% accuracy [17].

The ATLAS Magnet System

It contains three different magnetic systems: a thin solenoid inner diameter 2.46 m, thickness 5 cm, axial length 5.8 m, axial magnetic field 2 T at the center of the tracking volume around the inner tracking system, and 8 barrel and 2×8 endcap air-core toroid magnets magnetic fields between 0.5 T and 4 T, strongly varying with the radial distance from the toroid are arranged radially around the hadron calorimeters such that the Lorentz force bends charged tracks along their z coordinates. The toroid magnets do not affect the central solenoid field. All magnet systems are superconducting. Since there is a high magnetic field, highly energetic particles also curve enough so that their momentum is determined. The magnetic field is uniform in direction and the strength of the magnetic field allow to measurement of the momentum of the particles very accurately [18].

3.2.2 The CMS Detector

The CMS detector is another general purpose detector at the LHC. It is built around a huge solenoidal magnet. This cylindrical coil of superconducting wire can generates a magnetic field of 4 T. It is 21 m long, 15 m high and 15 m wide detector. It weighs 12,500 tons. For run II, it has been upgraded for higher energy and luminosity.

The CMS Inner Tracker

The tracker is designed to reconstruct the paths of highly energetic particles as well as to see tracks of short lived particles [19]. The tracker is made up of silicon only. The core of the detector which are the pixels deals with highest intense particles. The CMS silicon tracker has 14 layers in the endcaps and 13 layers in the central region [20]. The innermost three layers has 66 million in total pixels which are 100×150 micrometer in dimension. The next four layers has a 10 cm × 180 μm silicon strips, followed by remaining six layers of 25 cm × 180 μm strips It is used to reconstruct the path of highly energetic particles like muon, electron and hadrons very precisely. It can also see tracks coming from the decay of very short-lived particles such as "b quarks". By making accurate position measurement, to record particle paths, tracks are constructed by using a few measurement points. Each measurement is accurate to 10 μm.

The CMS Calorimeters

Like the ATLAS detector, the CMS calorimeter has two components - electromagnetic and hadronic. The electromagnetic calorimeter measures the energy of photons and electrons with high precision [21]. The electromagnetic calorimeter is made up of crystals of lead tungstate, $PbWO_4$. It has barrels section and two end caps which forms a layer between between the

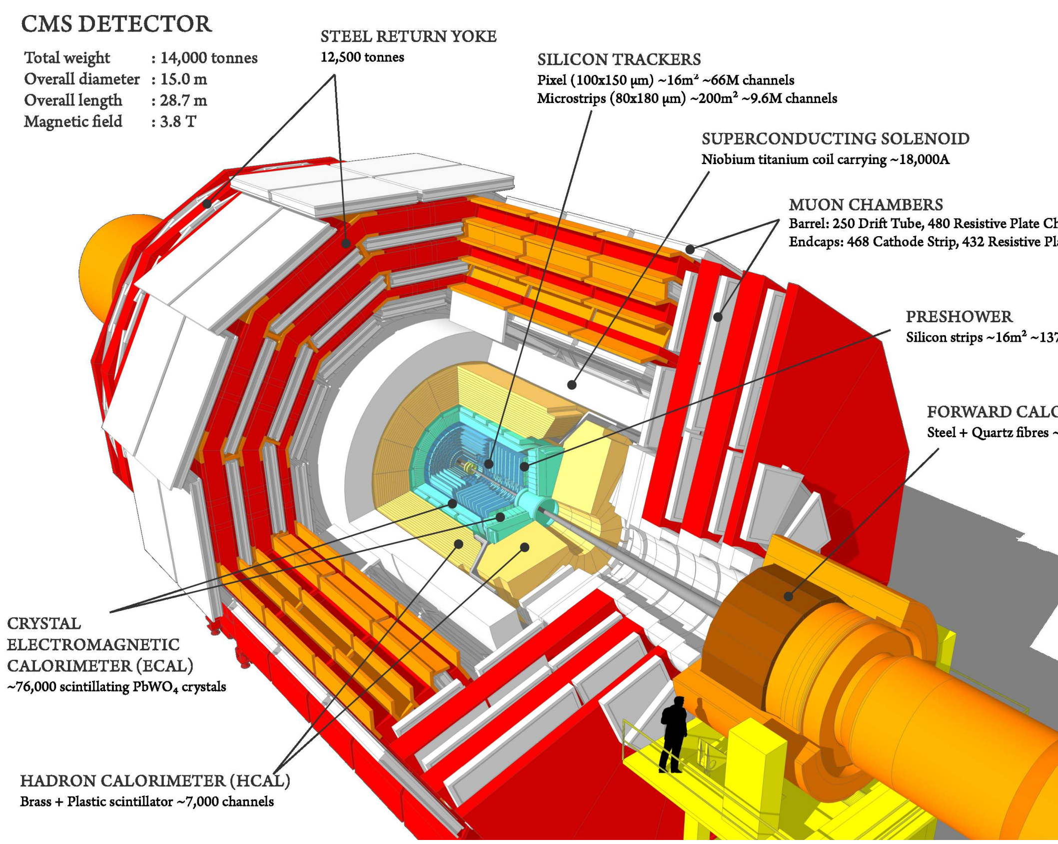

Figure 3.3: The schematic diagram of the CMS detector

hadronic calorimeter and the tracker. The cylindrical barrel has 61,200 crystals formed into 36 "supermodules". The ECAL is extremely dense but of optically clear material, which is used for stopping high energy particles. The lead tungstate crystal scintillates when electron or a photon passes through it. It produces light proportional to particles energy. For extra spatial precision, the ECAL also contains pre-shower detectors that sit in front of the endcaps. This allows the CMS to see the difference between single high energy photon and low energy photon.

The Hadronic Calorimeter is used for the measurement of energy of particles made up of gluons and quarks i.e. hadrons [22]. It also provide the information about the non-interacting particles like neutrinos [23]. It is made up of layers of dense material interleaved with tiles of plastic scintillators. The dense material and the plastic scintillators allow the maximum amount of absorbing material inside the magnet coil. Brass is used in the end caps of the calorimeter [24].

The CMS Magnet System

The CMS detector has a single, large solenoid magnet (axial length 12.9 m, thickness 60 cm and inner diameter 5.9 m). The magnet is used to fully immerse the inner tracking systems and hadronic calorimeters and electromagnetic calorimeters and in a 3.8 T axial magnetic field [25]. It also provides measurement of muon momentum via the 2 T field in the flux return yoke made out of 10,000 tonnes of steel. The job of the big magnet is to bend the paths of particles emerging from high-energy collisions in the LHC. The more momentum a particle has the less its path is curved by the magnetic field, so tracing its path gives a measure of momentum [26].

The CMS Muon Detector

To identify the muon particle and to measure the momentum of the muon, the CMS has three types of detectors, drift tubes, resistive plate chambers and the cathode strip chambers [27]. The drift tube is used to measure the precise trajectory in the central barrel region. The resistive plate chambers (RPC) gives a fast signal when muon passes through the muon detector. The Cathode strip chambers (CSC) are used in the end caps. The muon chambers are kept at the end part of the CMS detector where they can register their presence. Drift tube system measures muon positions in the barrel part of the detector [28]. Cathode strip chambers are used in the endcap disks where the magnetic field is very uneven and particle rates are very high. When a muon passes through a CSC or RPC, it knocks out an electron from the atom in its path and create an avalanche of electron. It helps in detecting muons.

3.3 Discovery Of the Higgs Boson

On July 4, 2012, there was a presentation at the CERN, with a press release "CERN experiments observe particle consistent with long-sought Higgs boson". According to the ATLAS experiment spokesperson Fabiola Gianotti "We observe in our data clear signs of a new particle, at the level of 5 sigma, in the mass region of around 126 GeV but little more time is needed to prepare these results for publication". According to the CMS collaboration spokesperson Joe Incandela." The results are preliminary but the 5 sigma at 125 GeV we are seeing is dramatic. This is indeed a new particle".

The results, that were presented, were based on the data collected in 2011 and 2012. Results were preliminary and the full data was still being analyzed. Main evidence for the Higgs boson came from the production process $gg \to H$ and its decay into rare decay channels $H \to \gamma\gamma$ and $H \to ZZ^*$. Looking at the mass distributions of photons and four leptons, one could observe the existence of the Higgs boson. The decay mode $H \to WW^*$ was also important. It was combination of data, which together was giving the strong evidence of the existence of the Higgs boson.

With more complete data analysis, now the existence of the Higgs boson has been established. March 14, 2013, CERN press release said, "New results indicate that particle discovered at CERN is a Higgs boson".

3.3.1 Discovery Of the Higgs Boson at the ATLAS

Argument for the discovery of the Higgs boson by the ATLAS collaboration [29] was based on the analysis of the dataset corresponding to the integrated luminosity of 4.8 fb^{-1} at the CM energy of 7 TeV, collected in 2011, and 5.8 fb^{-1} at CM energy of 8 TeV, collected in 2011 and 2012. They searched for the channels $H \to ZZ^* \to 4\ell$, $H \to \gamma\gamma$ and $H \to WW^*$. The previous analysis which was based on 7 TeV data for $H \to ZZ^* \to 4\ell$, $H \to \gamma\gamma$ $H \to WW^*$, $H \to b\bar{b}$ and $H \to \tau\tau$ were also used to strengthen the evidence. They found the evidence for the existence of a neutral boson with the mass of about 125 GeV. The observation had the combined significance of 5.9, corresponding to a background fluctuation probability of 1.7×10^{-9}. The observations were also compatible with the production and decay of the standard model Higgs boson.

The search of the standard model Higgs boson via its decay into the channel $H \to ZZ^* \to 4\ell$, where ℓ is either a electron or a muon, has a very good sensitivity over a range of Higgs boson mass between 110 GeV - 600 GeV. This is due to a very good momentum resolution of the ATLAS detector. The analysis comprises of selection/identification of two pairs of same flavor leptons with opposite sign. The expected cross-section is about 2.2 fb for the C.M. energy 7 TeV and 2.8 fb for the C.M. energy 8 TeV for a Higgs boson of mass 125 GeV for the process $H \to ZZ^* \to 4\ell$. The largest background comes from the continuum $(Z^*/\gamma^*)(Z/\gamma^*)$. For this range of the mass of the Higgs boson, there are other backgrounds, these are $Z + jets$ and $t\bar{t}$

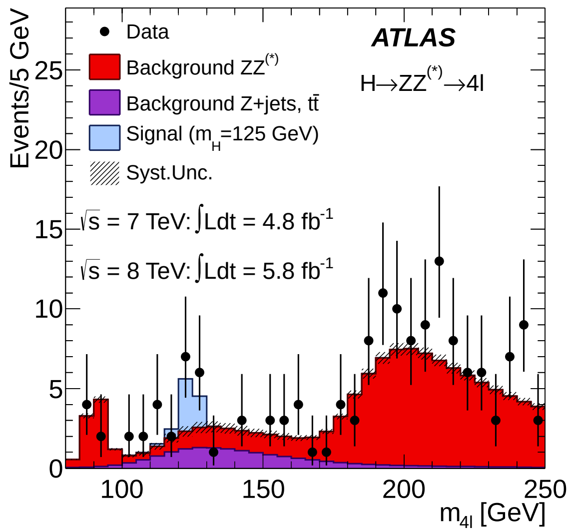

Figure 3.4: The distribution of the four-lepton invariant mass, $m_{4\ell}$, for the selected candidates, compared to the background expectation in the 80-250 GeV mass range, for the combination of the 7 TeV and 8 TeV data. The signal expectation for a SM Higgs with $m_H = 125$ GeV is also shown.

production. Here the charged lepton background arise from th decay of hadrons with b or c quark content or from mis-identification of a jet [29].

The expected distribution of $m_{4\ell}$ for the background and also for the Higgs boson signal with $m_H = 125$ GeV are compared to the data in Fig 3.1 [29]. The numbers of observed and expected events in a window of ±5 GeV around $m_H = 125$ GeV were presented for the combined 7 TeV and 8 TeV data. The distribution of the m_{34} versus m_{12} invariant mass is shown in Fig.3.2 [29].

The search of the Higgs boson through the decay $H \to \gamma\gamma$ was performed for the mass range 110 GeV and 150 GeV. The main background is the standard model diphoton production. The other contribution comes from the processes $\gamma + jet$, $jet + jet$, when one or two jets are mis-identified as photons. In this case also 7 TeV data was re-analyzed and merged with 8 TeV data. The distributions of the invariant mass, $m_{\gamma\gamma}$, of the diphoton events, summed over all categories, are shown in Fig.3.3 [29]. The result of a fit including a signal component fixed to $m_H = 126.5$ GeV and a background component is superimposed.

The signature of the channel $H \to WW^* \to e\nu\mu\nu$ has two opposite charged leptons with large transverse momentum and a large momentum mis-match due to escaping neutrinos. The dominant backgrounds are non-resonant WW, $t\bar{t}$, and Wt production, all of which have real W boson pairs in the final state. The other important backgrounds are $pp \to Z/\gamma^* \to \ell\ell$ with missing transverse energy which may arise from mis-measurement. The $W + jet$ events in which a jet fakes a electron/muon is also a background.The analysis presented in the paper was for 8 TeV center of mass energy in the mass range 110 GeV $< m_H <$ 200 GeV [30].

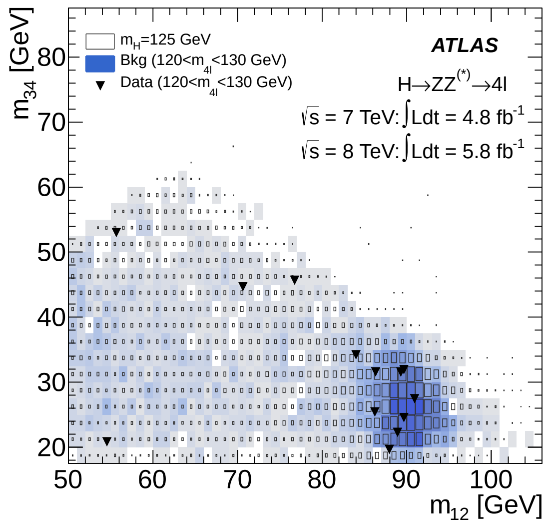

Figure 3.5: Distribution of the m_{34} versus the m_{12} invariant mass, before the application of the Z-mass constrained kinematic fit, for the selected candidates in the $m_{4\ell}$ range 120 − 130 GeV. The expected distributions for a SM Higgs boson with $m_H = 125$ GeV (the sizes of the boxes indicate the relative density) and for the total background (the intensity of the shading indicates the relative density) are also shown.

The mass of Higgs boson between the mass range 110 GeV - 582 GeV was excluded with 95% confidence level except some regions. The regions which were excluded with 95% confidence level are 111 GeV - 122 GeV and 131 GeV - 559 GeV. The mass regions excluded with 99% confidence level were 113 GeV - 114 GeV, 117 GeV - 121 GeV and 132 GeV - 527 GeV, while the expected exclusion range at 99% confidence level was about 113 GeV - 532 GeV.

For the combination of data at 7 TeV and 8 TeV, the largest local significance was found for the standard model Higgs boson with the mass hypothesis $m_H = 126.5$ GeV. The significance reaches a value of 6.0 σ. In the 2012 data, the maximum local significance of 4.9 σ was reached for the channels $H \rightarrow ZZ^* \rightarrow 4\ell$, $H \rightarrow \gamma\gamma$ and $H \rightarrow WW^* \rightarrow \ell\nu\ell\nu$. The channels $H \rightarrow ZZ^* \rightarrow 4\ell$ and $H \rightarrow \gamma\gamma$ were also showing an excess of events which had the highest mass resolution. While considering the full mass region of the search, 110 GeV - 600 GeV, for the value of $p_o = 1.7{\times}10^{-7}$ the global significance of the excess was obtained as 5.1 σ. The mass of the observed new particle for the process $H \rightarrow ZZ^*$ and $H \rightarrow \gamma\gamma$ is about 126 GeV.

The above discussed results gave an conclusive evidence for the discovery of a new particle with mass 126.0 GeV. The newly discovered particle decays to a pair of vector bosons. The vector bosons have the net electric charge zero which tells the newly discovered particle is a neutral boson. The spin-1 hypothesis was disfavored by the observation in the diphoton channel. The above results were compatible to the fact that the newly discovered particle was a Higgs boson. More complete analysis later confirmed the discovery.

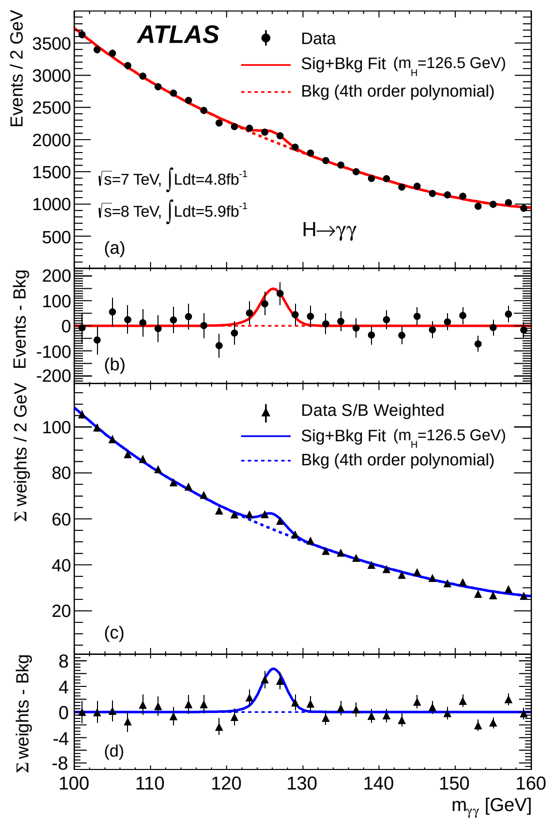

Figure 3.6: The distributions of the invariant mass of diphoton candidates after all selections for the combined 7 TeV and 8 TeV data sample. The inclusive sample is shown in (a) and a weighted version of the same sample in (c) The result of a fit to the data of the sum of a signal component fixed to $m_H = 126.5$ GeV and a background component is superimposed. The residuals of the data and weighted data with respect to the respective fitted background component are displayed in (b) and (d).

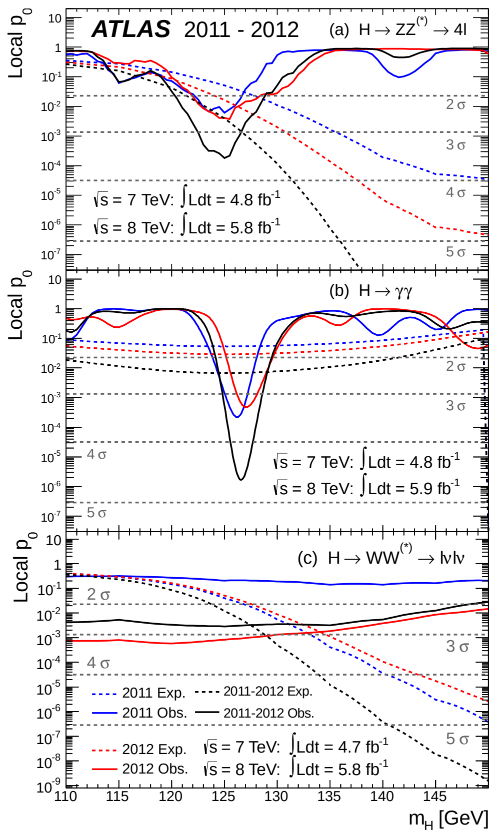

Figure 3.7: The observed local p_0 as a function of the hypothesized Higgs boson mass for the (a) $H \rightarrow ZZ \rightarrow llll$, (b) $H \rightarrow \gamma\gamma$ and (c) $H \rightarrow WW^* \rightarrow \ell\nu\ell\nu$ channels. The dashed curves show the expected local p_0 under the hypothesis of a SM Higgs boson signal at that mass. Results are shown separately for the $\sqrt{s} = 7$ TeV data (dark, blue), the $\sqrt{s} = 8$ TeV data (light, red) and their combination (black).

3.3.2 Discovery of the Higgs Boson at the CMS

At the same time, the results were also presented by the CMS collaboration. The database used was 5.1 fb^{-1} at 8 TeV CM energy. The searches were performed for the five decay modes: $H \rightarrow \gamma\gamma$, $H \rightarrow ZZ^*$, $H \rightarrow WW^*$, $H \rightarrow \tau\tau$ and $H \rightarrow b\bar{b}$. Previous searches by the CMS experiment had excluded the mass range 127 GeV - 600 GeV.

The CMS collaboration found the excess of events consistent with the production of a particle with mass 125 GeV. The observed local significance of the signal was 5 σ. The strongest evidence was $H \rightarrow \gamma\gamma$, with significance of 4.1 σ, followed by $H \rightarrow ZZ^*$ channel, with a significance of 3.2 σ

For the $H \rightarrow \gamma\gamma$ decay mode, the collaboration searched for a peak in the diphoton mass distribution in the range of 110 GeV - 150 GeV. This was on the top of irreducible direct production of two photons. The backgrounds were discussed in the last section. Apart from applying generic cuts to extract the events, a multivariate analysis, using boosted decision tree was also done. The events from the vector boson fusion process for the Higgs boson production were also included where in addition two jets were tagged. The CMS collaboration presented the results in terms of signal strength which was found to be 1.6 for 125 GeV Higgs boson. They also considered local p-value to show the existence of such a boson.

For the $H \rightarrow ZZ^*$ decay mode, the backgrounds are similar to that discussed in the case of the ATLAS searches. They selected again $ZZ \rightarrow 4\ell$ events in the range of 110 GeV $< m_{4\ell} <$ 160 GeV. The 4ℓ events consisted of 4e, 4μ and 2e+2μ. The background is very small. The CMS found the signal strength for this mode to be 0.7. Local p-value had a minimum at m_H= 125.6 GeV.The significance was 3.2 σ.

The CMS collaboration when combined the data for both the decay modes $H \rightarrow ZZ^*$ and $H \rightarrow 2\gamma$, a significance of 5 σ was achieved. Because of large backgrounds, the addition of $H \rightarrow WW^*$, $H \rightarrow b\bar{b}$ and $H \rightarrow \tau\tau$ signal events did not increase the significance. We note that the situation in last two years has significantly improved. Now decay modes $H \rightarrow WW^*$ and $H \rightarrow \tau\tau$ are also showing an excess of events over background events.

3.3.3 Study of the Spin and Parity of the Higgs Boson

Both CMS and ATLAS collaborations have analysed their data to determine the spin and parity of the detected particle [31, 32]. Both experiments have determined that it is a scalar particle, i.e., $J^P = 0^+$.

The ATLAS experiment studied the parity and spin quantum numbers [31] using the Higgs boson decay into the channels $H \rightarrow \gamma\gamma$, $H \rightarrow ZZ^* \rightarrow 4\ell$ and $H \rightarrow WW^* \rightarrow \ell\nu\ell\nu$, individually as well as the combination of the above. The analysis was done at the integrated luminosity of 20.7 fb^{-1} at the center of mass energy of 8 TeV. For the channel $H \rightarrow ZZ^* \rightarrow 4\ell$ data with integrated luminosity of 4.6 fb^{-1} at 7 TeV was also used. Because of the observation of the $H \to \gamma\gamma$ decay mode, the possibility of spin-1 was excluded by Landau-Yang theorem [33]. Still data was analysed by considering models for various spin-parity assignments. Angular correlations between decay products, angular, momentum and mass distributions favoured with very high confidence level the assignment of $J^P = 0^+$.

The CMS experiment [32] used 7 TeV and 8 TeV data with integrated luminosity of 17.3 fb^{-1}. They only looked at the decay channel $H \to ZZ^* \to 4\ell$. The spin and parity of the particle is sensitive to angular distribution of the lepton pair in this channel. The data was consistent with spin 0 hypothesis. Pure pseudoscalar hypothesis was not favoured.

3.4 Searches of the Other Production Mechanisms

The production mechanisms $pp \to VH$, where $V = W/Z$ [34, 35, 36, 37] and $pp \to ttH$ [38, 39, 40] have also been looked for by the both collaborations. For these mechanisms, most promising decay channel is $H \to b\bar{b}$. However, $H \to \gamma\gamma$ decay mode has also been searched for the ttH process.

The ATLAS experiment [35] has analysed its 7 TeV and 8 TeV data to search for the $pp \to VH$, where $V = W/Z$ processes, with $H \to b\bar{b}$. The W boson was decaying semileptonically, while Z could decay into leptons or neutrinos. The signal still does not have enough significance, only 1.4 (2.6) σ for $HW(Z)$ production. The CMS experiment [36, 37] has also analysed its data for decay modes similar to the ATLAS experiment. The most recent analysis has only a significance of 2.1 σ. However, it is clear that in the run II, both experiments would be able to observe this production mechanism.

The ATLAS experiment [38] has found no excess above the background for the ttH production. The CMS experiment [39, 40] experiment has made a more serious search using even neural net techniques to enhance the signal. They have also considered the pure hadronic decay channels also. This production mechanism is still to be established. However, as we show in this thesis, in the run II, this production mechanism should be observable.

3.5 The Status of the Higgs Boson Since July 2012

Since the July 4, 2012, announcement and accompanying papers, not only the discovery of the particle has been firmly established, but also its status as a standard model Higgs boson has been affirmed.

Both the collaborations have almost completely analysed their data for the production mechanism $gg \to H$ with the subsequent decay of the Higgs boson into decay channels $H \to \gamma\gamma, ZZ^*, WW^*, \tau\tau$ in detail [41, 42]. Some other rare decay channels $H \to \gamma Z, \mu\mu$ have also been looked for. Other major production mechanisms, vector boson fusion, VH production, and ttH production have also been searched. In these processes, the decay channel $H \to b\bar{b}$ has been looked for. The CMS and ATLAS experiments have also searched for some other rare decay modes of the Higgs boson also – $H \to \gamma Z, H \to \mu\mu$ [43, 44, 45, 46]. Because of very small branching ratios, only some bounds on the branching ratios have been placed.

The ATLAS collaboration has analysed its complete data set of about 25 fb^{-1} collected at 7 TeV and 8 TeV [41]. They have analysed all major production and decay mechanisms. The data set is consistent with the existence of a standard model Higgs boson of the mass 125.5 GeV with less than 0.5% uncertainty. Since then individual decay channels have been analysed in more details. The CMS collaboration has also done a complete analysis. They also find the discovered particle to be consistent with the standard model Higgs boson with mass of 125.02 GeV with less than 0.5 % uncertainty. The CMS experiment has also used decay channels $H \to ZZ^*, WW^*$ to rule out the existence of the Higgs boson between the mass range $127 - 710$ GeV [47].

Bibliography

[1] ALEPH, DELPHI, L3, OPAL Collaborations, and LEP Working Group for Higgs Boson Searches, Phys. Lett. B **565**, 61 (2003).

[2] ALEPH, CDF, D0, DELPHI, L3, OPAL, SLD Collaborations, the LEP Electroweak Working Group, the Tevatron Electroweak Working Group, and the SLD Electroweak and Heavy Flavour Groups, "Precision Electroweak Measurements and Constraints on the Standard Model", CERN PH-EP-2010-095, (2010).

[3] CDF and D0 Collaborations, Phys. Rev. Lett. **104**, 061802 (2010).

[4] L. Reina, Lectures on Higgs-Boson Physics, [arXiv:1208.5504].

[5] G. Aad *et al.* [ATLAS Collaboration], Phys. Lett. B **716**, 1 (2012); S.Chatrchyan *et al.* [CMS Collaboration], Phys. Lett. B **716**, 30 (2012).

[6] Andreas Hoecker, Commissioing and early physics analysis with the ATLAS and CMS experiments, [arXiv:1002.2891].

[7] http://www.atlas.ch/detector.html

[8] http://cms.web.cern.ch/

[9] http://www.atlas.ch/inner-detector.html

[10] ATLAS detector and physics performance : Technical Design Report 1, CERN-LHCC-99-14, ATLAS-TDR-14.

[11] ATLAS detector and physics performance : Technical Design Report 2, CERN-LHCC-99-15, ATLAS-TDR-15.

[12] M. Aleksa *et al.* JINST **3**, P06002 (2008).

[13] A. Atonin, *et al.* JINST **3**, P02010 (2008).

[14] D. Axen, *et al.* Rev. Sci. Instrum. **76**, 063306 (2005).

[15] ATLAS Collaboration-Technical design report, CERN-LHCC-97-22, ATLAS-TDR-10.

[16] S. Palestini, Nucl. Phys. Proc. Suppl., **125**, 337 (2003).

[17] C. Adorisio, *et al.* IEEE Trans. Nucl. Sci. **52**, 2971 (2005).

[18] ATLAS Collaboration-Technical design report, CERN-LHCC-97-18.

[19] Technical design report, http://cdsweb.cern.ch/record/368412; http://cds.cern.ch/record/368412/files/Tracker_TDR.pdf.

[20] J. L. Agram *et al.*, Nucl. Instrum. Meth. A **517**, 77 (2004).

[21] Kenneth Watson *et al.* IEEE Trans. Nucl. Sci. **51**, 228 (2004).

[22] http://cdsweb.cern.ch/record/349375; http://cds.cern.ch/record/349375/files/ECAL_TDR.pdf.

[23] http://cdsweb.cern.ch/record/357153; https://cmsdoc.cern.ch/ftp/TDR/HCAL/hcal.html.

[24] Banerjee, Sudeshna et al. Performance of Hadron Calorimeter with and without HO; CMS-NOTE-1999-063.

[25] G. Acquistapace *et al.*, http://cdsweb.cern.ch/record/331056, CERN-LHCC-97-010.

[26] A. Herv *et al.* IEEE Trans. Appl. Supercond **14**, 524 (2004).

[27] J. L. Agram *et al.*, Nucl. Instrum. Meth. A **517**, 77 (2004).

[28] http://cdsweb.cern.ch/record/343814; http://cds.cern.ch/record/343814/files/LHCC-97-032.pdf.

[29] G. Aad *et al.* [ATLAS Collaboration], [arXiv:1207.7214].

[30] G. Aad *et al.* [ATLAS Collaboration], Phys. Lett. B **716**, 62 (2012).

[31] G. Aad *et al.* [ATLAS Collaboration], [arXiv:1307.1432].

[32] S. Chatrchyan *et al.* [CMS Collaboration], [arXiv:1212.6639]. 307

[33] L. D. Landau, Dokl. Akad. Nauk, **60**, 207 (1948); C.-N. Yang, Phys. Rev. Lett. **77**, 242 (1950).

[34] G. Aad *et al.* [ATLAS Collaboration], [arXiv:1302.4403].

[35] G. Aad *et al.* [ATLAS Collaboration], [arXiv:1409.6212].

[36] S. Chatrchyan *et al.* [CMS Collaboration], [arXiv:1209.3937].

[37] S. Chatrchyan *et al.* [CMS Collaboration], [arXiv:1310.3687].

[38] G. Aad *et al.* [ATLAS Collaboration], [arXiv:1409.3122].

[39] S. Chatrchyan *et al.* [CMS Collaboration], [arXiv:1303.0763].

[40] S. Chatrchyan *et al.* [CMS Collaboration], [arXiv:1408.1682].

[41] G. Aad *et al.* [ATLAS Collaboration], [arXiv:1307.1427].

[42] S. Chatrchyan *et al.* [CMS Collaboration], Nature Phys., **10**, 557, (2014).

[43] G. Aad *et al.* [ATLAS Collaboration], [arXiv:1402.3051].

[44] S. Chatrchyan *et al.* [CMS Collaboration], [arXiv:1307.5515].

[45] G. Aad *et al.* [ATLAS Collaboration], [arXiv:1406.7663].

[46] S. Chatrchyan *et al.* [CMS Collaboration], [arXiv:1410.6679].

[47] S. Chatrchyan *et al.* [CMS Collaboration], [arXiv:1304.0213].

Chapter 4

Higgs Boson Production in Association with a Top Quark Pair

We consider the possible production of the Higgs boson in association with a top-quark pair and its subsequent decay into a tau-lepton pair or a W-boson pair. This process can give rise to many signatures of the Higgs boson. These signatures can have electrons, muons, tau jets, bottom jets and/or light flavor jets. We analyze the viability of some of these signatures. We will look at those signatures where the background is minimal. In particular, we explore the viability of the signatures "isolated 4 electron/muon" and "isolated 3 electron/muon + a jet" The jet can be due to a light flavor quark/gluon, a bottom quark, or a tau lepton. Of all these signatures, we find that "isolated 3 electron/muon + a tau jet", with an extra bottom jet, can be an excellent signature of this mode of the Higgs boson production. We show that this signature may be visible within a year, once the Large Hadron Collider (LHC) restarts. Some of the other signatures would also be observable after the LHC accumulates sufficient luminosity.

4.1 Introduction

In this chapter, we focus on the production mechanism $pp \to t\bar{t}H$, at $\sqrt{s}$= 14 TeV, with the subsequent decay of the Higgs boson into a tau-lepton pair [16], or a W-boson pair. There are enormous possibilities for a variety of signatures because there are many heavy particles in the final state which then decay into many more particles. In this letter, we will look at those signatures which have most leptons in the final state. More leptons in the final state means smaller background. However, it comes at the cost of fewer signal events. In a subsequent paper [17], we will analyze the signatures which have fewer leptons and more jets. There we will have more signal events, but larger background.

In the next section, we will discuss production, decay and signatures in a bit more detail. In the section 3, we would discuss the backgrounds. In the section 4, we would present numerical results. In the last section, we would conclude.

4.2 Production, Decay and Signatures

We are considering the production of the Higgs boson with a top-quark pair. This is fourth most important production mechanism. The process occurs through gluon-gluon or quark-quark annihilation. We will consider semileptonic decay of both the top quarks and the decay of the Higgs boson into a tau-lepton pair, or a W-boson pair. For the $M_H = 120 - 130$ GeV , the tau-lepton decay mode has a branching ratios of a $5 - 7$ percent. The tau-lepton can further decay into an electron/muon or hadrons and neutrinos. When it decays into hadrons, it manifest itself as a jet – tau jet. This jet has special characteristics compared to a quark/gluon jet. It is narrow and has very few hadrons. It is narrow because of the low mass of the tau lepton; it has few hadrons because tau lepton mostly has one-prong or three-prong decays. These properties of a tau jet can be used to distinguish it from a quark/gluon jet. The W-boson decay mode of the Higgs boson has a branching ratio of $14 - 30\%$ for the Higgs boson with the mass in the $120 - 130$ GeV range. Here both W-boson cannot be on-shell. The W-boson decays into leptons/quarks and neutrinos.

This production and decay chain can give rise to a multitude of signatures. The final state can have only jets, one electron/muon and jets, two electron/muon and jets, three electron/muon and jets and four electron/muon and jets. Some of these jets can be bottom jets or/and tau jets. Of all these signatures, because of the larger branching ratios, "only jets" signature will give rise to most signal events; but it will also have the largest background due to the production of the jets through the strong interaction processes. On the other hand, we have a signature of "4 electron/muon + jets". This signature has least number of signal events, but also the smallest background. One of the drawback of all these signatures is that one cannot reconstruct the Higgs boson mass through its decay products. This is because of the presence of many neutrinos in its decay products. However, as we will see, due to the manageable background, we can still identify the Higgs boson through these production and decay chains.

We shall consider the signature of " 4 electron/muon + jets" and "3 electron/muon + jets". Because of the small cross section for such events, due to small semileptonic branching ratios, we would minimize the number of jets to be observed. This will help us in increasing the number of signal events marginally, without increasing the background. So in the end, we shall be considering four signatures: "4 electron/muon", "3 electron/muon + a jet", "3 electron/muon + a tau jet", and "3 electron/muon + a bottom-jet". In this list, "3 electron/muon + a jet" will have largest signal events, while "4 electron/muon" will have the least number of signal events. We will also consider the signature "3 electron/muon" alone. The numerical results would be presented for three of these signatures, as the other two have large backgrounds.

Let us first consider the signature: "4 electron/muon". Such events occur when both the top quarks and tau leptons decay semileptonically. Such events also receive contributions when the Higgs boson (in $t\bar{t}H$ production) decays into 2 W-bosons. We will see that it makes larger contribution. Another contribution comes from the process $gg \to H$ and $H \to ZZ^*$. Such a contribution will be reduced if we veto events with a lepton pair of same flavor opposite charge (SFOC) which has mass close to the mass of the Z-boson. We have not included these events in the signature. Other signatures, with 3 electron/muon, occur when out of the top-quark pair and the tau-lepton pair, only three particles decay semileptonically; the remaining particle decays into hadrons/tau jet. These events also receive contribution from the decay $H \to WW^*$ after the ttH production. In this case, tau-lepton decay mode makes larger contribution. Because of the decay of the top quarks, these events naturally have bottom jets, irrespective of whether we observe them or not. We will find that observation of an extra bottom jet can increase the significance of a signature. We can also have a real tau jet in the signal events through the Higgs boson or a top-quark decay.

4.3 Backgrounds

All the signatures under consideration will receive contribution from the signal events, i.e. the production of the Higgs boson, and other SM processes which does not have a Higgs boson. Question is – is the background small enough to be sure that signal events have been produced ? To establish the viability of the signatures, we shall first identify the major background processes and then estimate their contributions. There are two classes of the backgrounds: (1) direct backgrounds, (2) mimic backgrounds. In the case of the direct background, the background processes produce events similar to the signal events. They have same particles as in the signal. On the other hand, mimic backgrounds have jets, which can mimic (fake) a tau jet, a bottom jet, or even an electron/muon. These mimic probabilities are usually quite small – less than a percent. So even if a background has large cross section, it becomes smaller when folded with mimic probability.

1. "4 electron/muon": There are many processes which can be backgrounds. The source of direct backgrounds are the processes $t\bar{t}Z, WWZ, WWWW, ZZ, t\bar{t}t\bar{t}$. The main sources of mimic backgrounds are: $WZ+$jet, $t\bar{t}W, WWW+$jet. These background occur when a jet mimics an electron/muon. As discussed below, the mimic backgrounds are not significant because of the very small probability of a jet to mimic an electron/muon, about 10^{-5} [41].

   Among the direct backgrounds, the most significant backgrounds would be due to the production of $t\bar{t}Z$ and ZZ events and subsequent decay into leptons. Using `MadGraph v5` [19], we find that the cross sections for the signal $t\bar{t}H$ is about 0.44 pb for $m_H = 125$ GeV, while the cross sections for $t\bar{t}Z$ and ZZ are 0.66 pb and 10.8 pb respectively. Because of very similar structure, $t\bar{t}Z$ will always be a significant background to the signal. These two backgrounds can be reduced by requiring appropriate $M_{\ell_1\ell_2}$ to be away from the mass of the Z-boson. But the background when a Z-boson decays into a tau-lepton pair and subsequent decay of the tau-leptons into electron/muon cannot be reduced in this way. These and the other values of the cross sections from MadGraph are with its default settings, unless stated otherwise. The processes $WWZ, WWWW,$ and $t\bar{t}t\bar{t}$ have the cross sections of about 100.0, 0.6 and 12.0 fb respectively. We clearly see that these processes are not important source of the backgrounds due to small cross sections.

2. "3 electron/muon + a jet": In this case, the direct backgrounds are $t\bar{t}Z, t\bar{t}W, ZZ, WZ +$ jet$, WWW +$jet$, WWZ$; the major mimic backgrounds are $t\bar{t}$ and $WW + 2$jet. As above, due to small probability of a jet faking an electron/muon, the mimic backgrounds can be ignored. Most of the direct backgrounds are self-explanatory. ZZ production is a background, when a Z-boson decays into a tau-lepton pair, and one of the tau leptons appears as a tau jet.

3. "3 electron/muon + a tau jet": In this case, the direct backgrounds are $t\bar{t}Z, t\bar{t}t\bar{t}, WWZ$; the major mimic backgrounds are $t\bar{t}, WZ +$jet$, WW + 2$ jet$, WWW +$jet$, t\bar{t}W$. As above, the backgrounds that fake an lepton are not important. But that backgrounds $WZ +$jet and $t\bar{t}W$ can be important where a light/bottom jet mimics a tau jet.

4. "3 electron/muon + a bottom jet": In this case, the direct backgrounds are $t\bar{t}Z, t\bar{t}W, t\bar{t}t\bar{t}$. In these processes the bottom jet would appear from a top-quark decay. The major mimic backgrounds are $t\bar{t}, WZ +$ jet$, WW + 2$ jet$, WWZ, WWW +$ jet$, t\bar{t}W$.

5. "3 electron/muon": There are many processes which can be backgrounds. The source of direct backgrounds are the processes $t\bar{t}Z, t\bar{t}W, WWZ, WWW, WZ, t\bar{t}t\bar{t}$. The main sources of mimic backgrounds are: $WW +$ jet$, t\bar{t}$. These background occur when a jet mimics an electron/muon.

4.4 Numerical results and Discussion

In this section, we are presenting numerical results. The signal and the background calculations have been done using `ALPGEN v2.14` [44] and its interface with `PYTHIA v6.325` [45]. Using `ALPGEN`, we generate the parton-level unweighted events. These events are then turned into more realistic events by hadronization, initial and final state radiation using `PYTHIA`. We have also applied following generic kinematic cuts:

$$p_T^{e,\mu,j} > 20 \text{ GeV}, \ |\eta^{\mathrm{e},\mu,\mathrm{j}}| < 2.5, \ \mathrm{R}(\mathrm{jj}, \ell\mathrm{j}, \ell\ell) > 0.4.$$

We have used CTEQ5L [46] parton distribution functions and other default parameters including renormalization and factorization scales. For the results, we have chosen the center-of-mass energy of 14 TeV and integrated luminosity is 100 fb^{-1}. We take mass of the top quark is

174.3 GeV. We are taking three different values for the mass of the Higgs boson – 120, 125 and 130 GeV.

One of our signatures has a tau jet. Both CMS and ATLAS collaborations [23] can identify tau jets. A tau jet is a manifestation of the hadronic decays of a tau lepton. A tau lepton has a branching ratios of approximately 65% to decay into hadrons. Two main characteristics of a tau jet are its narrowness and presence of only a few hadrons. These two features have been used to identify a tau jet. However, like the identification of a bottom jet, the identification of tau jet can only be done with some probability. The other jets due to quarks/gluon can also mimic a tau jet with small probability. Usually there is a trade-off between higher detection efficiency and higher rejection of the mimic-jets. We are taking two cases - one with high tau jet detection efficiency, other with low tau-detection efficiency. We are also presenting results by identifying a tau jet with an area-variable. This variable alone would not work well, as our number shows. The number of charge tracks will play a crucial role in discriminating a tau jet.

We are considering the detection of a bottom-jet also. We have used the identification probability (ϵ_b) of 55% [34, 35]. For other jets to mimic a bottom jet, we use the probability of 1%. For a jet faking a lepton, the probability is quite low. A light flavor jet can mimic a lepton with a probability of about 10^{-5}. For a bottom jet such a number is 5×10^{-5}. As we see in the signature, leptons comes either from the decay of a top-quark, or the decay of a tau-lepton, or a W-boson. So a pair of leptons would not have mass near the mass of a Z-boson. But a number of backgrounds have a Z-boson, so we use a cut of invariant mass of SFOC leptons: $|M_{\ell_1\ell_2} - M_Z| < 15$ GeV to reduce these backgrounds.

We are presenting the results for the three signatures: "3 electron/muon + a tau jet", "3 electron/muon + a bottom jet", and "4 electron/muon". In Table 1, we present the results for "3 electron/muon + a tau jet". For the signal events, the largest contribution comes from the tau-lepton decay channel of the Higgs boson. The Contribution of this channel is about 75%. The contribution of the W-boson decay channel is about 25%. Here we have considered four cases. In the first case, R-cut, we have used an area-variable of the tau jet cone, $R^{j^2}_{em}$ (adapted from [14]) to identify a tau jet. The behavior of the variable for the signal and backgrounds without normalization are displayed in Fig. 4.1. We clearly see that in the processes where there is a tau jet the variable is peaked towards a low value. We have checked that the area-variable gives better tau-jet efficiencies than the radius (R^{j}_{em}) [17]. We have used a cut of $R^{j^2}_{em} < 1 \times 10^{-4}$. As we are using only one characteristic of the tau jet, its narrowness, so it is not necessarily the best way [16]. We have tau-identification rate of 30% and mimic (rejection) rate of about 3%. In the second case of LTT, low tau-tagging, we have taken the low value for the tau-jet identification, 27%, and low mimic rate of 0.25%. Compared to the case 1, the signal decreases a bit and some of the backgrounds, specially $WZ + jet$ and $t\bar{t}W$ reduce significantly. Therefore, the significance of the signature increases. The case 3 of HTT [32], high tau-tagging, has high identification rate of 50% and the mimic rate of 1%. We see that the significance of the signature increases again. This is because of the larger number of signal events. In the case 4, we have used the fact that some of the backgrounds do not have a bottom jet for "free". So if we observe an extra bottom jet, i. e., the signature " 3 electron/muon + a tau jet + a bottom jet", then the background will reduce further, thus enhancing the significance of the signature. Since there are two bottom jets and only one is to be identified, we have used the identification probability of 80%. We will note that without identification of a jet some of the backgrounds would be higher by two-orders of magnitude, making the signal harder to observe. So identification of a jet play important role in reducing the backgrounds.

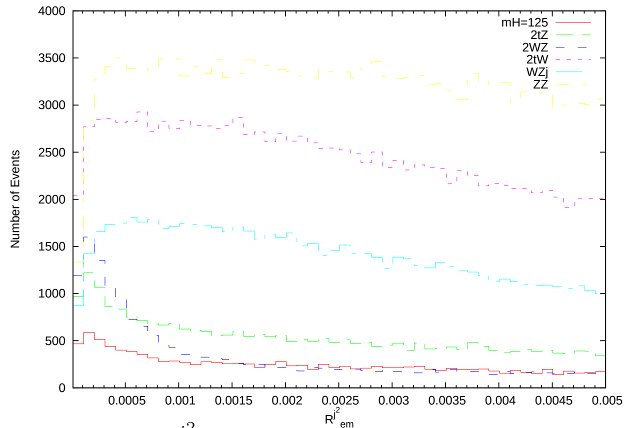

Figure 4.1: The profile of $R^{j^2}_{em}$ for the signal and major SM backgrounds.

In Table 2, we present the results for “3 electron/muon + a bottom-jet”. So we wish to identify a bottom jet instead of a tau jet. We now have fewer major backgrounds. But the $t\bar{t}W$ background increases by more than a order of magnitude. This is because this process has a bottom jet, and there is no need for this jet to mimic a tau jet. Therefore this is not an attractive signature, but with enough integrated luminosity, this signature can be observed.

In Table 3, there are results for the “4 electron/muon” signature. In this case, 75% of the events are through the W-boson decay channel of the Higgs boson; the rest are from the tau-lepton decay channel. We notice that this is an observable signature with a significance 3 – 5, depending on the mass of the Higgs boson. This signature is also obtained by the $gg \to H \to ZZ^*$ process [29]. So we also look for an extra bottom jet to make the signature exclusive for the $t\bar{t}H$ process. The major background is $t\bar{t}Z$ process. We see that the signature “ 4 electron/muon + a bottom-jet” is a useful signature with significance approaching 5 with 100 fb^{-1} of integrated luminosity.

τ jets id	Signal, M_H (GeV)			Backgrounds					$S/\sqrt{B}$, M_H (GeV)		
	120	125	130	$t\bar{t}Z$	WWZ	$t\bar{t}W$	WZj	ZZ	120	125	130
R-cut	22	20	19	14	2	12	24	7	2.9	2.6	2.5
LTT	20	18	17	13	2	1	2	6	4.1	3.7	3.5
HTT	37	33	32	23	3	4	10	12	5.1	4.6	4.4
B-tag/HTT	30	27	26	18	0	3	0	0	6.6	5.9	5.7

Table 4.1: Number of events for the signature "3 electron/muon + tau jet" at the LHC with the integrated luminosity of 100 fb^{-1} with the cuts and efficiencies specified in the text

Signal, M_H (GeV)			Backgrounds			$S/\sqrt{B}$, M_H (GeV)		
120	125	130	$t\bar{t}Z$	$t\bar{t}W$	WZj	120	125	130
42	34	26	26	312	6	2.3	1.8	1.4

Table 4.2: Number of events for the signature "3 electron/muon + bottom jet" at the LHC with the integrated luminosity of 100 fb^{-1} with the cuts and efficiencies specified in the text.

bottom jet id	Signal, M_H (GeV)			Backgrounds			$S/\sqrt{B}$, M_H (GeV)		
	120	125	130	$t\bar{t}Z$	WWZ	ZZ	120	125	130
no extra b	16	19	22	15	2	3	3.1	4.3	4.9
extra b	13	16	18	12	0	0	3.8	4.6	5.2

Table 4.3: Number of events for the signature "4 electron/muon" at the LHC with the integrated luminosity of 100 fb^{-1} with the cuts and efficiencies specified in the text

Bibliography

[1] G. Aad et al. [ATLAS Collaboration], Phys. Lett. B **716** 1 (2012).

[2] S. Chatrchyan *et al.* [CMS Collaboration], Phys. Lett. B **716**, 30 (2012).

[3] G. Aad *et al.* [ATLAS Collaboration], JHEP **1209**, 070 (2012).

[4] See for e.g., ATLAS Collaboration, ATLAS-CONF-2012-170.

[5] See for e.g., Pankaj Agrawal, Mod. Phys. Lett. A **16** , 897 (2001).

[6] The ATLAS collaboration, Phys.Lett. B **710**, 383 (2012).

[7] C. Kao and J. Sayre,Phys. Lett. B **722**, 324 (2013).

[8] S. Chatrchyan *et al.* [CMS Collaboration], Phys. Rev. Lett. **106**, 231801 (2011).

[9] S. Chatrchyan *et al.* [CMS Collaboration], Phys. Lett. B **713**, 68 (2012).

[10] The ATLAS collaboration, ATLAS-CONF-2012-160, ATLAS-CONF-2011-133.

[11] S.Fleischmann, http : //cds.cern.ch/record/1504815/files/CERN − THESIS − 2011 − 291.pdf; F.Scutti, http : //cds.cern.ch/record/1495356/files/ATL − PHYS − PROC − 2012 − 251.pdf; R. Prabhu, http://pi.physik.uni-bonn.de/pi_plone/lhc-ilc/theses/Thesis-PI-prabhu.pdf

[12] J. Baglio and A. Djouadi, arXiv:1103.6247 [hep-ph].

[13] See for e.g., Pankaj Agrawal, Mod. Phys. Lett. A **14**, 1479 (1999).

[14] See for e.g., The ATLAS collaboration, ATLAS-CONF-2013-080.

[15] See for e.g., CMS Collaboration,CMS-PAS-HIG-13-015.

[16] See for e.g., CMS Collaboration, JHEP **1305**, 145 (2013).

[17] Pankaj Agrawal, Somnath Bandopadhyay and Siba Prasad Das, in preparation.

[18] J. Alison, http://www.hep.upenn.edu/ johnda/Papers/vC/FakeFactorMethod.pdf

[19] F. Maltoni and T. Stelzer, JHEP **0302**, 027 (2003); J. Alwall, M. Herquet, F. Maltoni, O. Mattelaer, Tim Stelzer JHEP **1106**, 128 (2011).

[20] M.L. Mangano, M. Moretti, F. Piccinini, R. Pittau, A. Polosa, JHEP **0307**, 001 (2003).

[21] T. Sjostrand, S. Mrenna and P. Skands, JHEP **0605**, 026 (2006).

[22] H.L. Lai, J. Huston, S. Kuhlmann, J. Morfin, F. Olness, J.F. Owens, J. Pumplin and W.K. Tung, Eur. Phys. J. C **12**, 375 (2000).

[23] See for e.g., ATLAS Collaboration, in MSSM Higgs bosons, ATLAS-CONF-2011-132.

[24] See for e.g., CMS Collaboration, JINST **7**, P01001 (2012).

[25] See for e.g., CMS Collaboration, JINST **8**, P04013 (2012).

[26] See for e.g., exploiting b-tagging in CP-violating MSSM, Siba Prasad Das and Manuel Drees Phys. Rev. D **83** 035003 (2011) arXiv:1010.3701 [hep-ph]; Siba Prasad Das, Amitava Datta and Manuel Drees arXiv:0809.2209 [hep-ph].

[27] C. Englert, T. S. Roy and M. Spannowsky, Phys. Rev. D **84**, 075026 (2011).

[28] See for e.g., S. Dutta, Nucl. Phys. B (Proc. Supp.) **169**, 345 (2007).

[29] See for e.g., The ATLAS collaboration, ATLAS-CONF-2013-013.

Chapter 5

Dilepton Signatures of the Higgs Boson with Tau-jet Tagging

We consider the process $pp \to t\bar{t}H$. This process can give rise to many signatures of the Higgs boson. The signatures can have electrons, muons and jets. We consider the signatures that have two electrons/muons and jets. Tagging of a tau jet and a bottom jet can help reduce the backgrounds significantly. In particular, we examine the usefulness of the signatures "isolated 2 electrons/muons + a bottom jet + a tau jet", "isolated 2 electrons/muons + 2 tau jets", "isolated 2 electrons/muons + 2 bottom jets + a tau jet", and "isolated 2 electrons/muons + a bottom jet + 2 tau jets". We find that signatures with two tau jets are useful. The signatures with one tau jet are also useful, if we restrict to same-sign electrons/muons. These requirements reduce the backgrounds due the process with Z-bosons + jets and the production of a pair of top quarks. We show that these signatures may be visible in the run II of the Large Hadron Collider.

5.1 Introduction

The BEH mechanism of the Standard Model (SM) now seems to have been validated with the discovery of a Higgs boson like neutral scalar particle. The strong evidence has been presented by the both ATLAS [1] and CMS [2] Collaborations on the basis of the data taken in run I (2009-12) at the Large Hadron Collider (LHC). Because of the appearance of the signal in multiple channels, as seen by both collaborations, there is little doubt that the Higgs boson of the SM has been found. All channels of the discovery suggest a mass of about 125 GeV for the particle.

The LHC is now on a long shut-down to improve the luminosity and the center-of-mass energy. When it restarts to take data in 2015, one of its major goals would be to measure the couplings of the newly discovered Higgs boson to all the SM particles. This is specially important because of the prediction of the existence of scalar particles, sometime with properties similar to that of the SM Higgs boson, in various extensions and modifications of the standard model. To do so, one will need to identify the particle through multiple processes and measure the couplings of the scalar particle with various other SM particles. These couplings determine the branching ratios of the decay channels and also the production cross sections. Identification of the scalar particle through multiple processes will allow us to measure the couplings and confirm that the scalar particle is indeed the SM Higgs boson.

In this letter, we consider the production of the Higgs boson in association with a top-quark pair $pp \to t\bar{t}H$ [3, 4], with its subsequent decay into a tau-lepton pair or WW^*. As of now the Higgs boson has been primarily looked through its gluon-fusion production mechanism and then decay into channels $H \to \gamma\gamma$ [1, 2, 5], WW^* [6, 7], ZZ^* [8], and $\tau\tau$ [9, 10, 11, 12]. Various production mechanisms and the decay channels of the Higgs boson give rise to many signatures. Some of these signatures have already been discussed in the literature [13, 14, 15, 16, 17, 18, 19, 20, 21, 22, 23, 24, 25, 26, 27, 28, 29, 30]. In this letter, we focus on those signatures which have two electrons/muons (i.e., two electrons, or 2 muons, or one electron and one muon) and jets in the final state. These jets can be initiated by a light quark/gluons, a bottom quark, or a hadronic decay of a tau lepton (tau jet). It is experimentally possible to tag a jet from a bottom quark or a tau lepton. Such tagging helps in reducing the strong interaction backgrounds. One major source of the backgrounds is the production of a pair of top quarks with or without additional jets. One strategy to reduce this background would be to restrict the signature events to same-sign electrons/muons. We show the usefulness of this strategy, specially when only one jet is tagged as a tau jet.

In the next section, we will discuss the signatures that we consider. In the section 3, we will discuss the backgrounds to these signatures. In the section 4, we will present numerical results and some discussion. In the last section, we will conclude.

5.2 Signatures

We are considering a general class of signatures "2 electrons/muons + jets". As we see from Table 1, without any tagging of the jets, the backgrounds due to Z bosons + jets and $t\bar{t}$ + jets processes would overwhelm the signal. Therefore, to reduce the backgrounds, we are focusing on the signatures with two electrons/muons and at least two tagged jets. Since the top-quark background events always have bottoms jets, so to reduce it we will require at least one jet to be tagged as the tau jet. These signatures occur, when after the production of $t\bar{t}H$, the Higgs boson decays into a tau-lepton pair or WW^*. With these considerations, at least one of the top quark accompanying the Higgs boson decays semileptonically. The possibility of a top quark decaying into jets leads to an increase in the signal events, relative to when we have more than

2 electrons/muons in a signature. For the Higgs boson with a mass of $120 - 130$ GeV, the tau-lepton decay mode has a branching ratios of $5 - 7$ percent; the W-boson decay mode has a branching ratio of $14 - 30\%$. When a tau lepton decays into hadrons, it can manifest itself as a jet – tau jet. This jet has special characteristics. It is narrow and has very few hadrons. Its narrowness is due to the low mass of the tau lepton; it has few hadrons because a tau lepton decays into mostly 1 or 3 hadrons. These properties of a tau jet help us to distinguish it from a quark/gluon jet. There is usually a $25 - 50\%$ efficiency to tag a tau jet. The probability of a light quark/gluon jet to mimic a tau jet can be taken to be $1 - 0.1\%$ [31, 32, 33]. A bottom jet is broader than a light quark/gluon jet and has more particles. It can mimic a tau jet less often. A bottom jet can be identified with a probability of about $50 - 60\%$, while other jets can mimic it with a probability of about one percent [34, 35, 36].

To manage the background and at the same time to keep the signal events to a sufficiently high level, we are analyzing the signatures "2 electrons/muons + a tau jet + a bottom jet", "2 electrons/muons + two tau jets","2 electrons/muons + a tau jet + two bottom jet", and "2 electrons/muons + two tau jet + a bottom jet". In the signal, the bottom jets appear due to the decay of the top quarks; a tau jet can occur due to the decay of the Higgs boson, or the decay of the on-shell/off-shell W bosons from the Higgs boson or the top quarks. Electrons/muons can appear due to a decay chain of the Higgs boson, or the decay of the top quarks. Presence of electrons/muons in a signature is important to reduce the background. Recently, we had considered the signatures with three or four electrons/muons [38]. We saw that the presence of a bottom jet with four electrons/muons and the presence of one additional tau jet and a bottom jet with three electrons/muons help in keeping the background low enough to be able to detect the signal.

In the case of two electrons/muons, as we will see, it will be useful to have either at least two tau jets or one tau jet with only same sign electrons/muons in the signatures. Either of these two strategies will reduce the signal events, but will reduce the backgrounds even more. We can have same sign charged leptons in the signature because there are three/four on-shell/off-shell W boson in the production and decay chains under considerations. Two of these W-bosons can produce the same-sign electrons/muons. Sources of off-shell W-bosons can be tau-lepton, which can come from the decays of the Higgs boson, the top quark, the W-boson, or the Z-boson. This strategy of observing same-sign leptons will significantly reduce the large background from the production of a top quark pair with or without jets and Z + jets. Z + jets backgrounds are significantly reduced or eliminated due to the the tagging of at least 2 jets as tau and/or bottom jets. This tagging also reduces the top-quark pair production background to the same-sign lepton signatures. This is discussed more in the next section.

5.3 Backgrounds

All the signatures under consideration will get contribution from the signal events, i.e. the production of the Higgs boson, and other SM processes which do not have a Higgs boson. To establish the viability of the signatures for signal detection, we shall first identify the main background processes and then estimate their contributions. We will consider both types of the backgrounds: direct backgrounds and mimic backgrounds. In the case of the direct background, the background processes produce events similar to the signal events. They have same particles as in the signal. On the other hand, mimic backgrounds have jets, which can mimic (fake) a tau jet, a bottom jet, or even an electron/muon. These mimic probabilities are usually quite small – less than a percent. So even if a background has large cross section, it becomes smaller when folded with mimic probabilities. Tagging efficiencies and mimic probabilities were discussed in the last section.

One important type of background occurs when a B-meson in a bottom jet decays into an electron/muon and this lepton is away from the jet. This leads to an extra lepton in the event. Possibility of such backgrounds has been explored in the literature [37]. As we have argued [38], such backgrounds which can occur due to the top quark production is not significant for the signatures under consideration. This is mainly due to two facts – (1) we have at least one tau jet in the signatures, so backgrounds are to be folded with the tau jet mimic probability; this reduces the backgrounds significantly, (2) the electrons/muons in our signatures are hard and have same minimum transverse momentum as the bottom jet from which they might have separated; the $p_T^{\ell,b} > 20$ GeV. Let us now discuss the backgrounds to the signatures.

1. "2 electrons/muons + a tau jet + a bottom jet": There are many processes which can be backgrounds. The source of major direct backgrounds is the process $t\bar{t}Z$. The main sources of mimic backgrounds are: $t\bar{t}, WZ +$ jet$, t\bar{t}W, Z + 2$ jets$, WW + 2$ jets. We are not considering backgrounds when a jet mimics an electrons/muons. Such mimic backgrounds are not significant because of the very small probability of a light jet to mimic an electron/muon, about $10^{-4} - 10^{-5}$ [39, 40, 41, 42, 43].

   Among the direct backgrounds, the most significant backgrounds would be due to the production of $t\bar{t}Z$ and subsequent decay into leptons. Because of similar structure, $t\bar{t}Z$ will always be a significant background to the signal. This background can be reduced by requiring appropriate $M_{\ell_1\ell_2}$ to be away from the mass of the Z-boson. But the background when a Z-boson decays into a tau-lepton pair and the subsequent decay of the tau-leptons into electrons/muons cannot be reduced in this way. The major mimic background is the production of a top-quark pair. Even with the folding of mimic probabilities, it remains large enough to make the signature almost not useful. However, when we consider the subset of events with same-sign electrons/muons, this signature becomes quite viable. This is because now the $t\bar{t}$ process is no longer a significant background.

2. "2 electrons/muons + two tau jets" : In this case, the direct backgrounds are the processes $t\bar{t}Z, WWZ, ZZ$. The main sources of mimic backgrounds are: $t\bar{t}, WZ +$ jet$, t\bar{t}W, Z + 2$ jets$, WW + 2$ jets. Presence of two tau jets will be crucial to reduce the mimic backgrounds.

3. "2 electrons/muons + a tau jet + 2 bottom jets": The source of major direct backgrounds is the processes $t\bar{t}Z$. The main sources of mimic backgrounds are: $t\bar{t} +$ jet$, 2WZ +$

jet, $t\bar{t}W, Z +$ 3 jets, $WW +$ 3 jets. These backgrounds are similar to that of the first signature, except that some mimic backgrounds have an extra jet.

4. "2 electrons/muons + a bottom jet + 2 tau jets": The sources of major direct backgrounds are the processes $t\bar{t}Z, WWZ, ZZ$. The main mimic backgrounds are: $t\bar{t}+$ jet, $2WZ +$ jet, $t\bar{t}W, Z + 3$ jets, $WW + 3$ jets. These backgrounds are similar to that of the second signature, except that some mimic backgrounds have an extra jet.

5.4 Numerical results and Discussion

In this section, we are presenting numerical results and discussion of the results. The signal and the background events have been calculated using ALPGEN (v2.14) [44] and its interface with PYTHIA (v6.325) [45]. Using ALPGEN, we generate parton-level unweighted events. Using the PYTHIA interface, these events are then turned into more realistic events by hadronization, initial and final state radiation. We have applied following kinematic cuts:

$$p_T^{e,\mu,j} > 20 \text{ GeV}, \ |\eta^{\mathrm{e},\mu,\mathrm{j}}| < 2.5, \ \mathrm{R}(\mathrm{jj}, \ell\mathrm{j}, \ell\ell) > 0.4.$$

We are presenting results for the three different values of M_H – 120, 125 and 130 GeV. We have used the default values for the parameters including renormalization and factorization scales. For the parton distribution functions, we have used CTEQ5L [46] distribution. We have chosen the center-of-mass energy of 14 TeV and integrated luminosity of 100 fb^{-1}. The mass of the top quark is 174.3 GeV.

We are presenting the results for four signatures: "2 electrons/muons + a tau jet + a bottom jet", "2 electrons/muons + two tau jets","2 electrons/muons + a tau jet + two bottom jet", and "2 electrons/muons + two tau jet + a bottom jet". For the bottom jet, we have used the identification probability of 55% [34, 35]. For other jets to mimic a bottom jet, we use the probability of 1%. For a tau jet, we consider two cases. This is because of a trade-off between higher detection efficiency and higher rejection of the mimic-jets. In the first case of LTT, low tau-tagging, we have taken the low value for the tau-jet identification, 30%, and low mimic rate of 0.25% [31]. The second case of HTT [32], high tau-tagging, has high identification rate of 50% and higher mimic rate of 1%. To reduce the Z boson related backgrounds, we have required the missing transverse momentum to be more than 25 GeV and applied a cut on the mass of same-flavor and opposite-sign lepton pair by requiring $|M_{\ell_1\ell_2} - M_Z| > 15$ GeV. We have smeared the jet/lepton energies using the energy resolution function

$$\frac{\Delta E}{E} = \frac{a}{\sqrt{E}} \oplus b, \tag{5.1}$$

where $\oplus$ means addition in quadrature. For the jets $a = 0.5$ and $b = 0.03$. For the electrons/muons we take $a = 0.1$ and $b = 0.007$. Since we are not using the mass of two or more jets, inclusion of jet energy resolution does not affect the results significantly. Lepton energy resolution is quite good, so the results are also not significantly impacted.

In Table 1, we display results with only basic kinematic cuts with the observation of only two electrons/muons. The table has results for the signal events and various possible backgrounds. There are two cases of same-sign (SS) electrons/muons and opposite-sign (OS) electrons/muons. These events may or may not have a tau or a bottom jet. This table illustrates the importance of jet tagging and observing same-sign electrons/muons. First we note that there is marginal differences in the two-electrons and two-muons events. This is primarily statistical, i. e., due to the finite event sample. We also notice large backgrounds due to Z boson processes and top-quarks only processes. A missing p_T cut and a cut on the mass of the lepton pair will help in reducing these backgrounds. Fig 1 illustrates the importance of the missing p_T cut. We also notice the virtual elimination of the background due to a top-quark pair production for the same-sign electrons/muons. However, it will come at the cost of reducing the signal events by a factor of about 3. In the case of only one tau jet in the signature, one will have to adopt this strategy. For the two tau jets case, the extra rejection factor, due to the observation of the second tau jet, can reduce the backgrounds by about a two orders of magnitude, so the restriction to same-sign electrons/muons is not necessary.

In the Tables 2-5, we present results for various signatures for the integrated luminosity of 300 fb^{-1}. This is the expected luminosity for the run II. We have included only the major backgrounds. We have also taken into account Next-to-leading-order (NLO) contributions to the signal and background processes. To do so, we have multiplied the leading-order (LO) results by appropriate K-factors. The K-factor is taken as 1.20 for the $t\bar{t}H$ [47] process; the K-factors for the $t\bar{t}Z$ [48], $t\bar{t}W$ [49], and ZZ [50] are taken to be 1.35. The K-factor for the $WZ+$jet [51] is chosen as 1.3, while for the WWZ [52] production, it is 1.7. For the processes $t\bar{t}$ [53] and $t\bar{t}+$ jet [54], K-factors are taken to be 1.5 and 1.4 respectively. For the $Z + 2$ jet, the K-factor is 1.3 [55]. Because of the smaller K-factor for the signal, as compared to the backgrounds, its inclusion increases the significance only marginally.

In Table 2, we present the results for "2 electrons/muons + a tau jet + a bottom-jet". So we wish to identify a bottom jet and a tau jet. We note that for the different masses of the Higgs boson, the number of signal events are almost identical. This is because as M_H increases, the branching ratio $H \to \tau\tau$ decreases, but it increases for $H \to WW^*$. This together with different kinematics of the electrons/muons from these two decay modes lead to nearly same events for different M_H. For example, for the $M_H = 125$ GeV case, the contribution of the WW^* decay mode is about 32%, but for $M_H = 130$ GeV it is 60%. The signal events for this signature are the largest of all the considered signatures. This happens in part due to the appearance of only one tau jet. With 2 pairs of W boson decaying into only three leptons, it gives rise to an additional combinatorial factor that increases the signal events. This signature has very large background from the $t\bar{t}W$ and $t\bar{t}$ processes. The significance is not good for both the LTT and HTT cases. However, if we restrict to the same-sign electrons/muons in the signature, the signature's significance becomes more than 6, making it a pretty good signature.

Process	$e\mu$		ee		$\mu\mu$		$\ell\ell$		
	SS	OS	SS	OS	SS	OS	SS	OS	Total
$t\bar{t}H$ (120 GeV)									
$H \to \tau\tau$	49.6	103.2	26.3	46.6	27.8	51.8	103.7	201.6	305.3
$H \to WW^*$	81.6	173.0	40.4	86.7	41.2	89.5	163.2	349.2	512.4
$t\bar{t}H$ (125 GeV)									
$H \to \tau\tau$	44.6	82.7	21.2	42.2	20.9	43.1	86.7	167.9	254.6
$H \to WW^*$	116.3	245.0	57.6	121.2	59.4	123.7	233.4	489.9	723.3
$t\bar{t}H$ (130 GeV)									
$H \to \tau\tau$	33.4	65.8	16.8	32.5	17.9	33.4	68.1	131.7	199.8
$H \to WW^*$	150.0	315.2	72.9	153.5	77.2	162.4	300.1	631.1	931.3
$t\bar{t}Z$	125.9	158.7	62.4	845.7	62.5	886.9	250.8	1891.2	2142.0
WWZ	21.5	156.0	10.4	194.8	10.4	203.0	42.3	553.8	596.2
ZZ	228.6	474.9	116.6	34448.9	111.0	35783.0	456.2	70706.8	71163.0
$t\bar{t}$	147.5	668973.8	98.3	334339.4	49.2	343632.1	295.0	1346945.3	1347240.3
$t\bar{t}j$	3.5	502156.5	0.0	245773.5	3.5	255277.5	7.0	1003207.5	1003214.5
$t\bar{t}W$	471.6	920.8	223.9	450.2	244.9	458.4	940.4	1829.5	2769.9
$Z2j$	0.0	36207.8	0.0	4900649.0	0.0	5019321.2	0.0	9956178.0	9956178.0
$Z3j$	0.0	9668.3	0.0	1382073.3	0.0	1441322.7	0.0	2833064.2	2833064.2
$WWZj$	23.0	159.5	10.7	204.7	10.6	204.8	44.3	569.0	613.3
ZZj	113.1	221.6	49.2	14930.5	49.2	15479.5	211.6	30631.6	30843.2
ZZW	7.3	8.1	3.7	92.4	3.8	96.9	14.8	197.4	212.2

Table 5.1: Number of Dilepton events for 100 fb^{-1} integrated luminosity. The results for different flavor compositions with same-sign (SS) and opposite-sign (OS)

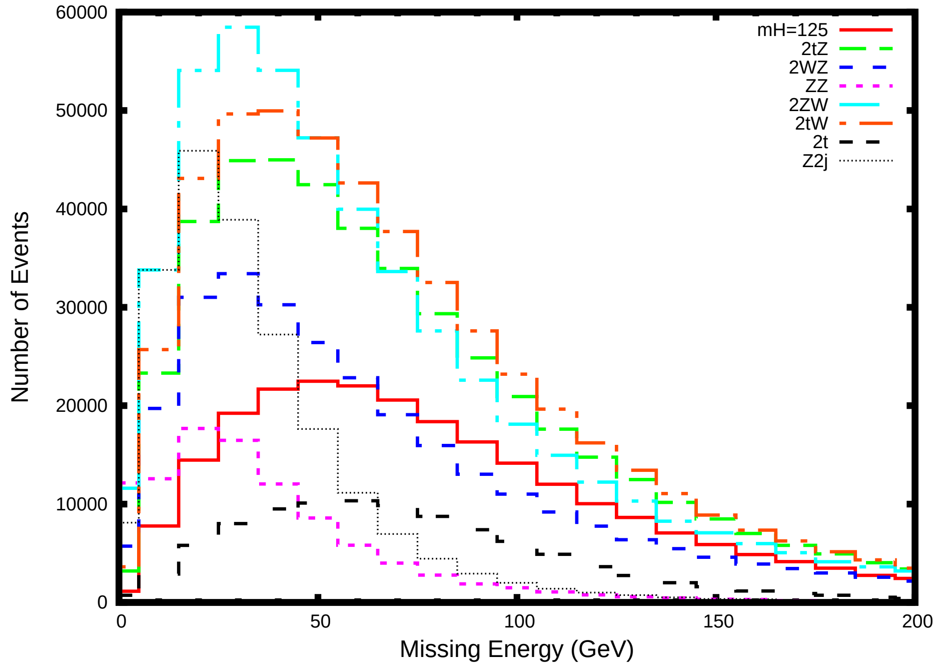

Figure 5.1: Distribution of missing p_T for the signal and the major SM backgrounds.

In Table 3, we present the results for the signature "2 electrons/muons + two tau jets". The major backgrounds are $t\bar{t}Z, t\bar{t}, ZZ$, and $Z+2$ jets. Significance for the 125 GeV Higgs boson is 4.0 for the HTT case. Because of the reduction in the signal events, LTT case is not as useful. As we see, restricting to the same-sign electrons/muons is again not useful due to a paucity of events. We can also identify an additional bottom jet. This reduces the number of signal events, but this also leads to a significant reduction in the Z boson backgrounds. As we see from Table 4, this signature of "2 electrons/muons + two tau jets + a bottom jet" has a very good significance.

In the Table 5 we display the results for the signature "2 electrons/muons + a tau jet + two bottom jets". Here signal events are smaller as compared to that in Table 2. This is due to the identification of an additional bottom jet. As there, here the background due to the production of a top-quark pair is quite large. However, if we observe only the same-sign electrons/muons, the significance may reach the observational value within the run II of LHC.

τ jets id	Signal, M_H (GeV) 120	125	130	Backgrounds $t\bar{t}Z$	$t\bar{t}$	$t\bar{t}W$	$Z2j$	$S/\sqrt{B}$, M_H (GeV) 120	125	130
LTT	333	333	330	336	8228	567	30	3.4	3.4	3.4
HTT	555	552	549	561	32889	942	120	2.9	2.9	2.9
SS/LTT	111	111	111	111	9	189	0	6.3	6.3	6.3
SS/HTT	186	183	183	186	3	315	0	8.3	8.2	8.2

Table 5.2: Number of events for the signature "2 electrons/muons + a tau jet + a bottom jet" with the integrated luminosity of 300 fb^{-1} with cuts and efficiencies specified in the text.

τ jets id	Signal, M_H (GeV) 120	125	130	Backgrounds $t\bar{t}Z$	WWZ	$t\bar{t}W$	$t\bar{t}$	$Z2j$	ZZ	$S/\sqrt{B}$, M_H (GeV) 120	125	130
LTT	42	41	37	36	6	3	9	9	30	4.4	4.3	3.8
HTT	117	114	104	111	15	9	147	276	84	4.6	4.5	4.1
SS/LTT	14	14	12	12	3	0	0	0	0	3.6	3.6	3.1
SS/HTT	39	38	35	36	6	3	0	0	0	5.8	5.7	5.2

Table 5.3: Number of events for the signature "2 electrons/muons + 2 tau jets" with the integrated luminosity of 300 fb^{-1} with the cuts and efficiencies specified in the text.

τ jets id	Signal, M_H (GeV) 120	125	130	Backgrounds $t\bar{t}Z$	$t\bar{t}W$	$t\bar{t}j$	$S/\sqrt{B}$, M_H (GeV) 120	125	130
LTT	34	33	30	30	3	6	5.4	5.3	4.8
HTT	93	91	83	90	6	81	6.9	6.8	6.2
SS/LTT	11	11	10	10	0	0	3.5	3.5	3.2
SS/HTT	31	30	28	30	3	0	5.4	5.2	4.9

Table 5.4: Number of events for the signature "2 electrons/muons + 2 tau jets + a bottom jet" with the integrated luminosity of 300 fb^{-1} with the cuts and efficiencies specified in the text.

τ jets id	Signal, M_H (GeV)			Backgrounds			$S/\sqrt{B}$, M_H (GeV)		
	120	125	130	$t\bar{t}Z$	$t\bar{t}j$	$t\bar{t}W$	120	125	130
LTT	126	126	123	129	2286	213	2.4	2.4	2.4
HTT	210	210	207	213	9141	357	2.1	2.1	2.1
SS/LTT	42	42	42	43	0	72	4.0	4.0	4.0
SS/HTT	70	70	69	71	0	120	5.0	5.0	5.0

Table 5.5: Number of events for the signature "2 electrons/muons + a tau jet + two bottom jets" with the integrated luminosity of 300 fb^{-1} with the cuts and efficiencies specified in the text.

Let us now comment on the possible uncertainties in the above results [3]. Theoretically, the main sources of uncertainties are choices of parton distribution functions, factorization and renormalization scales. In obtaining our results, we have used the NLO cross sections. These cross sections have the uncertainties of the order $10 - 15\%$. Furthermore, when these choices increase/decrease the signal cross section, they also correspondingly increase/decrease the background cross sections. Therefore, there is a further reduction in the uncertainties due to the cancellation when we compute the significance – a ratio. Overall, one may expect only a few percent theoretical uncertainty in the significance of the signatures. Similarly, there will be cancellation of uncertainties due to experimental limitations. Therefore, our results about the significance are quite robust.

Bibliography

[1] G. Aad et al. [ATLAS Collaboration], Phys. Lett. B **716**, 1 (2012).

[2] S. Chatrchyan *et al.* [CMS Collaboration], Phys. Lett. B **716**, 30 (2012).

[3] S. Chatrchyan *et al.* [CMS Collaboration], JHEP **1305**, 145 (2013).

[4] See for e.g., Pankaj Agrawal, Mod. Phys. Lett. A **16**, 897 (2001).

[5] See for e.g., ATLAS Collaboration, ATLAS-CONF-2012-170.

[6] S. Chatrchyan *et al.* [CMS Collaboration], [arXiv:1312.1129 [hep-ex]].

[7] C. Kao and J. Sayre, Phys. Lett. B **722**, 324 (2013).

[8] The ATLAS collaboration, Phys. Lett. B **710**, 383 (2012).

[9] G. Aad *et al.* [ATLAS Collaboration], JHEP **05**, 070 (2012).

[10] S. Chatrchyan *et al.* [CMS Collaboration], Phys. Rev. Lett. **106**, 231801 (2011).

[11] S. Chatrchyan *et al.* [CMS Collaboration], Phys. Lett. B **713**, 68 (2012).

[12] The ATLAS collaboration, ATLAS-CONF-2012-160, ATLAS-CONF-2011-133.

[13] S. Dittmaier *et al.* [LHC Higgs Cross Section Working Group Collaboration], [arXiv:1101.0593 [hep-ph]].

[14] C. Englert, T. S. Roy and M. Spannowsky, Phys. Rev. D **84**, 075026 (2011).

[15] S.Fleischmann, http : //cds.cern.ch/record/1504815/files/CERN − THESIS − 2011 − 291.pdf; F.Scutti, http : //cds.cern.ch/record/1495356/files/ATL − PHYS − PROC − 2012 − 251.pdf; R. Prabhu, http://pi.physik.uni-bonn.de/pi_plone/lhc-ilc/theses/Thesis-PI-prabhu.pdf

[16] See for e.g., S. Dutta, Nucl. Phys. B (Proc. Suppp.) **169**, 345 (2007).

[17] J. Baglio and A. Djouadi, [arXiv:1103.6247 [hep-ph]].

[18] D. Curtin, J. Galloway and J. G. Wacker, Phys. Rev. D **88**, 093006 (2013). [arXiv:1306.5695 [hep-ph]].

[19] N. Craig, M. Park and J. Shelton, [arXiv:1308.0845 [hep-ph]]; A. Belyaev and L. Reina, JHEP **0208**, 041 (2002).

[20] P. Onyisi, R. Kehoe, V. Rodriguez and Y. Ilchenko, [arXiv:1307.7280 [hep-ex]].

[21] E. Contreras-Campana, N. Craig, R. Gray, C. Kilic, M. Park, S. Somalwar and S. Thomas, JHEP **1204**, 112 (2012). N. Craig, J. A. Evans, R. Gray, C. Kilic, M. Park, S. Somalwar and S. Thomas, JHEP **1302**, 033 (2013).

[22] A. Carmona, M. Chala and J. Santiago, JHEP **1207**, 049 (2012).

[23] A. Azatov and A. Paul, [arXiv:1309.5273 [hep-ph]].

[24] M. R. Buckley, T. Plehn, T. Schell and M. Takeuchi, [arXiv:1310.6034 [hep-ph]].

[25] J. Ellis, D. S. Hwang, K. Sakurai and M. Takeuchi, JHEP **1404**, 004 (2014).

[26] C. Englert, A. Freitas, M. Muhlleitner, T. Plehn, M. Rauch, M. Spira and K. Walz, [arXiv:1403.7191 [hep-ph]].

[27] A. Greljo, J. F. Kamenik and J. Kopp, [arXiv:1404.1278 [hep-ph]].

[28] See for e.g., P. Agrawal, Mod. Phys. Lett. A **14**, 1479 (1999).

[29] P. Agrawal and S. D. Ellis, Phys. Lett. B **229**, 145 (1989).

[30] P. Agrawal, D. Bowser-Chao and K. -M. Cheung, Phys. Rev. D **51**, 6114 (1995).

[31] C. Kao, D.A. Dicus, R. Malhotra, Y. Wang, Phys. Rev. D **77** 095002 (2008).

[32] See for e.g., CMS Collaboration, JINST **7**, P01001 (2012).

[33] G. Bagliesi, [arXiv:0707.0928 [hep-ex]].

[34] See for e.g., CMS Collaboration, JINST **8**, P04013 (2012).

[35] See for e.g., exploiting b-tagging in CP-violating MSSM, S. P. Das and M. Drees Phys. Rev. D **83** 035003 (2011), [arXiv:1010.3701 [hep-ph]]; Journal of Physics: Conference Series **259**, 012071 (2010); S. P. Das, A. Datta and M. Drees, [arXiv:0809.2209 [hep-ph]].

[36] M. Lehmacher, [arXiv:0809.4896 [hep-ex]].

[37] Z. Sullivan and E. L. Berger, Phys. Rev. D **82**, 014001 (2010).

[38] P. Agrawal, S. Bandyopadhyay and S. P. Das, Phys. Rev. D **88**, 093008 (2013).

[39] G. Aad *et al.* [ATLAS Collaboration], JINST **3**, S08003 (2008).

[40] D. Curtin, J. Galloway, J. G. Wacker, Phys. Rev. D **88**, 093006 (2013).

[41] J. Alison, https://cds.cern.ch/record/1536507.

[42] G. Aad *et al.* [ATLAS Collaboration], Phys. Rev. D **87**, 052002 (2013).

[43] G. Aad *et al.* [ATLAS Collaboration], Eur. Phys. J. C **71**, 1577 (2011).

[44] M.L. Mangano, M. Moretti, F. Piccinini, R. Pittau, A. Polosa, JHEP **0307**, 001 (2003).

[45] T. Sjostrand, S. Mrenna and P. Skands, JHEP **0605**, 026 (2006).

[46] H.L. Lai, J. Huston, S. Kuhlmann, J. Morfin, F. Olness, J.F. Owens, J. Pumplin and W.K. Tung, Eur. Phys. J. C **12**, 375 (2000).

[47] W. Beenakker, S. Dittmaier, M. Kramer, B. Plumper, M. Spira and P. M. Zerwas, Nucl. Phys. B **653**, 151 (2003).

[48] A. Lazopoulos, T. McElmurry, K. Melnikov and F. Petriello, Phys. Lett. B **666**, 62 (2008).

[49] J. M. Campbell and R. K. Ellis, JHEP **1207**, 052 (2012).

[50] J. M. Campbell and R. K. Ellis, Phys. Rev. D **60**, 113006 (1999).

[51] F. Campanario, C. Englert, S. Kallweit, M. Spannowsky and D. Zeppenfeld, [arXiv:1006.0390 [hep-ph]].

[52] V. Hankele and D. Zeppenfeld, Phys. Lett. B **661**, 103 (2008).

[53] E. Laenen, J. Smith and W.L. van Neerven, Nucl. Phys. **B 369**, 1992 (543); E.L. Berger and H. Contopanagos, Phys. Rev. D **54**, 1996 (3085); S. Catani, M.L. Mangano, P. Nason and L. Trentadue, Nucl. Phys. B **478**, 273 (1996).

[54] S. Dittmaier, P. Uwer, and S. Weinzierl, Phys. Rev. Lett. **98**, 262002 (2007).

[55] J. M. Campbell and R. K. Ellis, Phys. Rev. D **65**, 113007 (2002).

Chapter 6

Summary

This thesis is about the signatures of the Higgs boson through the production mechanism $pp \to t\bar{t}H$. We have considered the Higgs boson decay channels $H \to \tau\tau, WW^*$. This production and decay chain gives rise to a number of different signatures. Some of these signatures have been analyzed in this thesis. Remaining are under study. In particular, we have analyzed the two, three and four lepton signatures. We have emphasized the need to tag tau-jet to control the backgrounds. We find that in the run II of the LHC, these signatures may be visible.

In the first chapter, we gave an introduction to the electroweak model with some discussion on the weak interaction before gauge theory, and the construction of the electroweak $SU(2) \times U(1)$ theory. We also saw how the Lagrangian of the electroweak model was developed. Then we discussed strong interaction and put together the standard model Lagrangian.

In the second chapter, we saw some of the production mechanisms of the Higgs boson, its decay modes and its major signatures. In this chapter, we discussed the production of the Higgs boson by four different mechanisms, i.e. via gluon fusion, via weak vector boson fusion, Higgs-Strahlung process and in association with a heavy quark pair. We then discussed the major decay modes and some rare decay modes. Combining the production mechanisms and the decay modes we got some of the possible signatures which we discussed briefly.

In the third chapter, We discussed some elementary aspects of the LHC. Two main general purpose detectors at the LHC are the ATLAS and CMS. Theses detectors have been used in the discovery of the Higgs boson and are being used to find any signs of the physics beyond the standard model. We discussed major components of these detectors. Finding the Higgs boson has been a major achievement of the LHC. Its discovery was anounced on July 4, 2012. Subsequent analysis has confirmed its existence. In this chapter, we have discussed the discovery of the Higgs boson by the ATLAS collaboration in some detail. We also mentioned the discovery by the CMS collaboration and what has happened since the discovery.

The fourth and fifth chapters describe the research work done and form the heart of the thesis. In the fourth chapter, we considered the production of the Higgs boson with a top-antitop quark pair. The Higgs boson decays into a pair of tau leptons or a pair of W bosons and we get distinctive signatures of the Higgs boson. The signatures contain electrons/muons, tau jets, bottom jets and/or light flavor jets. We did analysis of some of these signatures and found that some of the signatures can have good significance. In particular, we have analyzed the signatures "isolated 4 electron/muon" and "isolated 3 electron electron/muon + a jet'. The jet may arise due to a light flavor quark/gluon, a bottom jet or a tau jet. When these signatures were analyzed, we saw that "isolated 3 electron/muon + a tau jet", with an extra bottom jet can be an excellent signature to detect the Higgs boson. It can have a significance of 5.9, considering the mass of the Higgs boson as 125 GeV and an integrated luminosity of 100 fb^{-1}. We also found that some other signatures like "4 electron/muon + bottom jet", "3 electron/muon + a bottom jet" and "4 electron/muon" are expected to be observable at the LHC.

In the fifth chapter, we have again considered the process $pp \rightarrow t\bar{t}H$ and the same decay channels. In this chapter, our focus was on dilepton signatures with jets. Our analysis again illustrated the importance of the tau-jet tagging. We have analysed the signatures, "isolated 2 electrons/muons + a bottom jet + a tau jet", "isolated 2 electrons/muons + 2 tau jets","isolated 2 electrons/muons + 2 bottom jets + a tau jet", and "isolated 2 electrons/muons + a bottom jet + 2 tau jets". We found that the signatures containing two or a single tau jet are useful to reduce the background. In the case of a single tau jet, the event should have same sign leptons. The major backgrounds are the production of top quark and processes with Z boson. The above defined requirements are useful to suppress the background with Z-bosons + jet and also the background which is due to the generation of a top quark pair. For the second and the forth signature the significance is quiet good and the processes can be seen in LHC run II. The other two signatures have large background due to top-quark pair production. But if we restrict ourselves to same sign electron/muon the above two signatures may be visible.

Currently, we are working on single lepton + jets and multijet signatures. It appears that in the case of single lepton, three tau jets need to be tagged, while for the multijet signature, four tau jets needs to tagged. This work is in progress.